ASTROBIOLOGY
Volume 8, Number 1, 2008

DOI: 10.1089/ast.2007.0134

Research Paper

Microbial Rock Inhabitants Survive Hypervelocity Impacts on Mars-Like Host Planets: First Phase of Lithopanspermia Experimentally Tested

GERDA HORNECK,[1] DIETER STÖFFLER,[2] SIEGLINDE OTT,[3] ULRICH HORNEMANN,[4] CHARLES S. COCKELL,[5] RALF MOELLER,[1,6] CORNELIA MEYER,[1,2] JEAN-PIERRE DE VERA,[3] JÖRG FRITZ,[2] SARA SCHADE,[2] and NATALIA A. ARTEMIEVA[7,8]

ABSTRACT

The scenario of lithopanspermia describes the viable transport of microorganisms via meteorites. To test the first step of lithopanspermia, *i.e.*, the impact ejection from a planet, systematic shock recovery experiments within a pressure range observed in martian meteorites (5–50 GPa) were performed with dry layers of microorganisms (spores of *Bacillus subtilis*, cells of the endolithic cyanobacterium *Chroococcidiopsis*, and thalli and ascocarps of the lichen *Xanthoria elegans*) sandwiched between gabbro discs (martian analogue rock). Actual shock pressures were determined by refractive index measurements and Raman spectroscopy, and shock temperature profiles were calculated. Pressure-effect curves were constructed for survival of *B. subtilis* spores and *Chroococcidiopsis* cells from the number of colony-forming units, and for vitality of the photobiont and mycobiont of *Xanthoria elegans* from confocal laser scanning microscopy after live/dead staining (FUN-I). A vital launch window for the transport of rock-colonizing microorganisms from a Mars-like planet was inferred, which encompasses shock pressures in the range of 5 to about 40 GPa for the bacterial endospores and the lichens, and a more limited shock pressure range for the cyanobacterium (from 5–10 GPa). The results support concepts of viable impact ejections from Mars-like planets and the possibility of reseeding early Earth after asteroid cataclysms. Key Words: Lithopanspermia—Impact—Shock pressure—Ejecta—Microbial survival—Interplanetary transfer of life. Astrobiology 8, 17–44.

[1]German Aerospace Center DLR, Institute of Aerospace Medicine, Köln, Germany.
[2]Museum für Naturkunde, Humboldt-Universität zu Berlin, Berlin, Germany.
[3]Institut für Botanik, Heinrich-Heine-Universität, Düsseldorf, Germany.
[4]Ernst-Mach-Institut für Kurzzeitdynamik, Fraunhofer-Gesellschaft, Freiburg, Germany.
[5]Open University, Milton Keynes, United Kingdom.
[6]German Collection of Microorganism and Cell Cultures GmbH (DSMZ), Braunschweig, Germany.
[7]Institute for Dynamics of Geospheres, Russian Academy of Science, Moscow, Russia.
[8]Planetary Science Institute, Tucson, Arizona.

1. INTRODUCTION

ASTEROID AND COMET IMPACTS on Earth are commonly viewed as causes of catastrophic destructions to the biosphere, be it on local or global scales (Ryder *et al.*, 1996; Sleep *et al.*, 1989; Maher and Stevenson, 1988; see also Cockell *et al.*, 2006). However, some models consider scenarios where life may have avoided annihilation by escaping its home planet via impact-ejected rocks (Sleep and Zahnle, 1998) and making a return after conditions have improved (Wells *et al.*, 2003) or being transported to another habitable planet (Mileikowsky *et al.*, 2000; Gladman *et al.*, 2005). The latter process has been termed "lithopanspermia," in reference to the theory of "panspermia," which was formulated by Arrhenius (1903). While panspermia postulates that microscopic forms of life, such as spores, can be dispersed in space by the radiation pressure from the Sun and, thereby, seed life from one planet to another, lithopanspermia assumes that impact-expelled rocks serve as transfer vehicles for microorganisms that colonize those rocks (Melosh, 1988).

The theoretical possibility of the transfer of life, by meteorites, between early Mars and Earth during the period of heavy bombardment has been proposed (Gladman, 1997; Mileikowsky *et al.*, 2000). Some observations are consistent with this possibility, such as the recent discoveries that protracted occurrences of water existed on the ancient surface of Mars, which suggests a habitable early surface (Squyres *et al.*, 2004), and the observed transfer of rocks between Mars and Earth, as confirmed by about 40 martian meteorites found on Earth to date (Melosh, 1984; Vickery and Melosh, 1987; Weiss *et al.*, 2000; Nyquist *et al.*, 2001; Head *et al.*, 2002; Artemieva and Ivanov, 2004; Fritz *et al.*, 2005). These martian meteorites consist exclusively of igneous rocks, including volcanic and plutonic varieties such as basalts, feldspathic lherzolites, pyroxenites, and dunites. Their crystallization ages are predominantly young and reveal some distinct groupings at about 180 Ma, 300–600 Ma, and 1300 Ma with only one plutonic meteorite that crystallized about 4500 Ma ago (Nyquist *et al.*, 2001). Petrographic studies on shock metamorphism of martian meteorites (Fritz *et al.*, 2005) and numerical simulations of the impact-induced ejection of martian rocks beyond the escape velocity of Mars have demonstrated a launch window for martian meteorites from about 5–10 GPa up to about 55 GPa (Artemieva and Ivanov, 2004; Fritz *et al.*, 2005).

Of course, viable transfer from one planet to another requires that microorganisms survive not only the escape process, *i.e.*, ejection into space by the impact of a cosmic projectile (asteroid, comet) on the parent planet, but also the journey through space, *i.e.*, timescales in space comparable with those experienced by the martian meteorites, which range between 1 and 20 million years (Eugster *et al.*, 1997; Nyquist *et al.*, 2001). Microorganisms would have to survive the entry process as well (Mileikowsky *et al.*, 2000; Clark, 2001).

In a variety of space experiments, the survival of microorganisms during a hypothetical space journey has been studied (*e.g.*, Horneck *et al.*, 1984, 1994, 1995, 2001a; Mancinelli *et al.*, 1998). It has been found that spores of *Bacillus subtilis* survive the hostile environment of space for at least 6 years, provided they are shielded against the harmful solar UV radiation (Horneck *et al.*, 1994). Taking into account the probability of survival of bacterial spores with respect to radiation damage, DNA decay by hydrolysis, or vacuum exposure, Mileikowsky *et al*. (2000) showed in a quantitative study that natural transfer of viable microbes from Mars to Earth or vice versa, via rocks greater than 1 m in size is a highly probable process that could have occurred many times during the history of our Solar System. However, single bacterial spores, as suggested by the original panspermia hypothesis (Arrhenius, 1903), would be killed by the energetic solar UV radiation within a few minutes (Horneck *et al.*, 2001a).

So far, little is known about whether rock-inhabiting microbial communities would survive the stress of an impact ejection. Except for some provisional studies on vegetative bacteria and bacterial endospores (Horneck *et al.*, 2001b; Burchell *et al.*, 2001, 2003, 2004; Willis *et al.*, 2006), no systematic shock recovery experiments have been done with rock-inhabiting microbial communities hosted in appropriate martian analogue rocks.

We report here on a systematic study of the survival rates of resistant terrestrial microorganisms embedded in a martian analogue rock (gabbro) at the pressure range indicated by the martian meteorites. Microbial representatives (bacterial spores, epilithic and endolithic microbial communities) were selected as described in the following.

Bacterial endospores have been recognized as the hardiest known forms of life on Earth and can

FIG. 1. ***Chroococcidiopsis*** **in its natural environment, colonizing a rock in the Negev Desert as a thin endolithic film.**

withstand extremely hostile conditions in the dormant state (reviewed in Nicholson *et al.*, 2000). The high resistance of *Bacillus* endospores is mainly due to a dehydrated, highly mineralized core enclosed in thick protective envelopes, the cortex and the spore coats, and the saturation of their DNA with small, acid-soluble proteins (Setlow, 1994). Spores of *Bacillus subtilis* have served as a model system for the study of the likelihood of interplanetary transfer in space experiments (Apollo 16, 17; ASTP; Spacelab 1; D1, D2; IML1, IML2; LDEF; EURECA; MIR; FOTON; Shuttle S/MM 03, 05, 06; STS6) (*e.g.*, Horneck *et al.*, 1994, 2001a), sounding rockets (Fajardo-Cavazos *et al.*, 2005), as well as in laboratory experiments that simulate certain phases of lithopanspermia (*e.g.*, Horneck *et al.*, 2001b; Benardini *et al.*, 2003; Burchell *et al.*, 2004, Nicholson *et al.*, 2006).

The desiccation-resistant, ionizing radiation-resistant phototroph *Chroococcidiopsis* is thought to be one of the most extreme-tolerant cyanobacteria. The unicellular, non-motile cyanobacterium is found in hot deserts, such as the Negev Desert in Israel, and cold deserts like the Ross Desert of the Antarctic (Friedmann and Ocampo-Friedmann, 1985; Büdel and Wessels, 1991). In its natural environment, the organism often colonizes microscopic fissures (chasmoendoliths) and structural cavities (cryptoendoliths) of rocks (Fig. 1), or it forms biofilms at the stone-soil interface under pebbles of desert pavements (hypoliths, *sensu* Golubic *et al.*, 1981). Thus we considered it a good model organism for impact-shock experiments. Because water in hot deserts is available for just a few days a year, the organism has evolved to cope with prolonged desiccation stress (Grilli Caiola *et al.*, 1993), and it is tolerant to UV radiation (Cockell *et al.*, 2005).

The lichen *Xanthoria elegans* is a characteristic colonizer of high mountain regions (Fig. 2) and particular sites in polar regions, where it is well adapted to environmental extremes, such as large temperature fluctuations, extreme desiccation, and intense UV radiation (Green *et al.*, 1999). The high resistance of lichens to environmental extremes is mainly due to a densely structured upper cortex (de Vera *et al.*, 2003, 2004), secondary lichen metabolites such as parietin that screen against UV radiation (Solhaug *et al.*, 2003; Solhaug and Gauslaa, 2004; Wynn-Williams *et al.*, 2002), lichen-specific antioxidants (Kranner *et al.*, 2005); and a gelatinous matrix (Belnep *et al.*, 2001; Flemming and Wingender, 2001). *Xanthoria elegans* has shown a very high resistance to the harsh environment of space during space simulation studies (de la Torre *et al.*, 2002; de Vera *et al.*, 2003; 2004) and in a recent open space experiment (Sancho *et al.*, 2007). These characteristics suggest *Xanthoria elegans* as one of the most resistant eukaryotic organisms and a suitable candidate for studies on the likelihood of lithopanspermia.

The aim of this study has been to tackle the question of whether, and to what extent, endolithic microorganisms ejected by impact processes might survive conditions such as those experienced by the martian meteorites: shock pressures of about 5–55 GPa and post-shock temperature increases of about 1 K up to 1000 K, respectively. The data

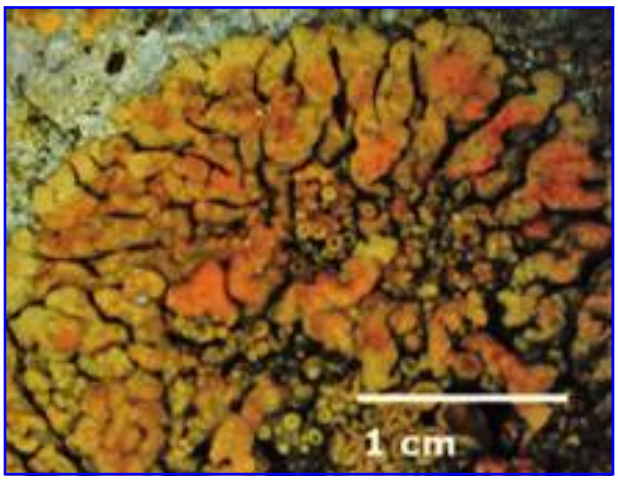

FIG. 2. ***Xanthoria elegans*** **colonizing a rock in the Alps (Seiser Alm, South Tyrol, Italy, GPS N46°54′, E11°62′) (Photo: J.P. de Vera).**

provide a realistic estimate of the likelihood of the first stage of the hypothesis of lithopanspermia, *i.e.*, the viable transport of life between planets (Mars and Earth, in particular), by means of rocks ejected through impact processes. Regardless of whether evidence of life is eventually found on Mars, this work elucidates the general physical plausibility of the transfer of life from Mars-like planets to other habitable planets within star systems.

2. MATERIALS AND METHODS

2.1. Shock recovery experiments and selected peak shock pressures

To expose host rocks with different types of endolithic and epilithic microorganisms to peak shock pressures in the range observed in martian meteorites—typically from 5 to 55 GPa (Fritz *et al.*, 2005; Bischoff and Stöffler, 1992)—we used 2 different plane wave impact techniques, the high-explosive technique and the air gun plane wave impact technique, of the Ernst-Mach-Institut für Kurzzeitdynamik at Freiburg i. Br., Germany (Müller and Hornemann, 1969; Arnold, 1988). In these devices, a plane metal plate is accelerated to velocities of some 0.5–2.6 km/s, which impacts a metal container that holds a test sample composed of a layer of microorganisms that are sandwiched between 2 thin discs of rock. The complete device including the sample is depicted in Fig. 3.

This type of shock recovery experiment is based on the so-called reverberation technique, *i.e.*, the peak shock pressure in the sample is achieved via multiple reflections of the shock wave at the metal container–rock interfaces. The device and the reverberation technique are described in previous papers (*e.g.*, Müller and Hornemann, 1969; Stöffler and Langenhorst, 1994; Horneck *et al.*, 2001b) and are further detailed in the Appendix. The desired peak shock pressure, which is produced by the impact of the flyer plate, can be varied by changing the values

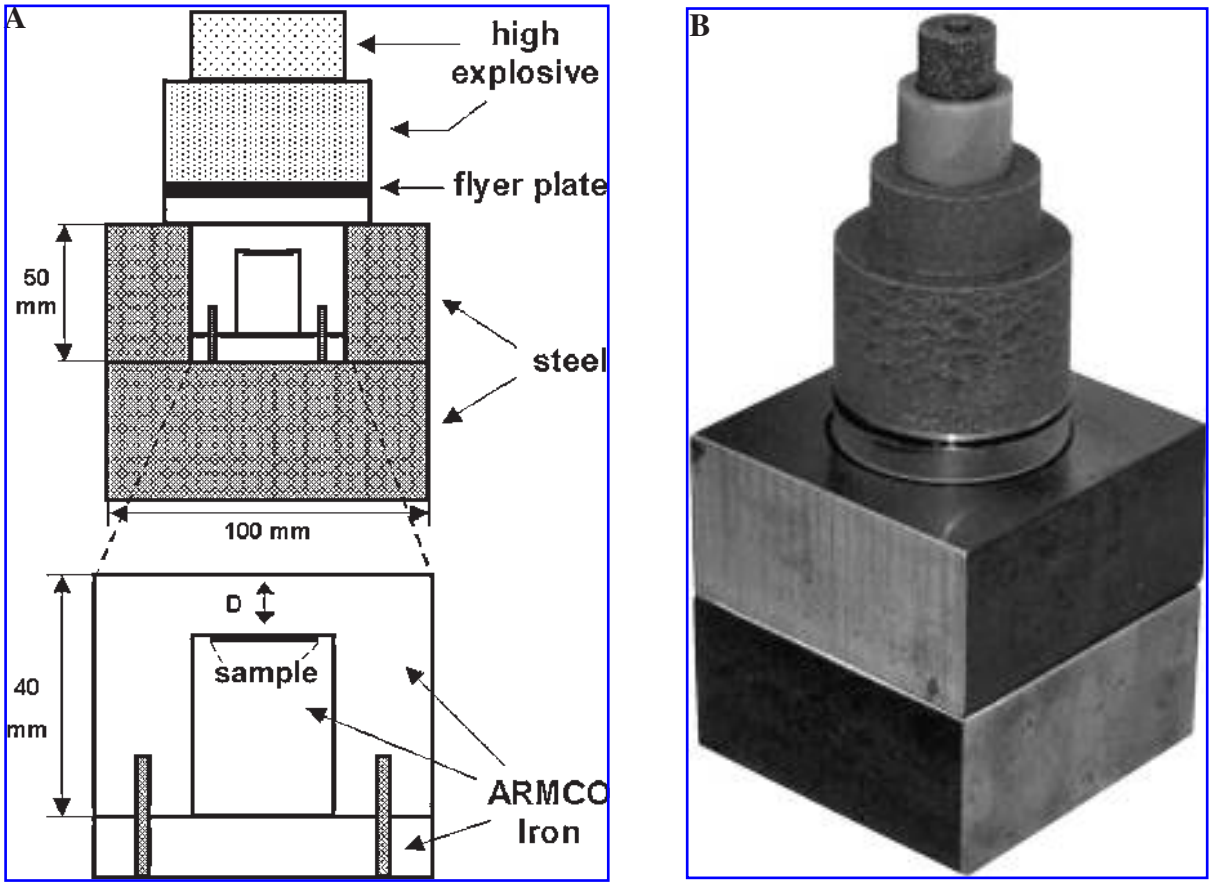

FIG. 3. Sketch (A) and photo (B) of the high-explosive device for shock-recovery experiments.

of *d* (thickness of the flyer plate) and *D* (distance of the sample to the surface) and the type of explosive. The correlation between *d*, *D*, and the shock pressure has been calibrated previously in separate calibration runs with electrical pins for various types of explosives (see details in Müller and Hornemann, 1969; Stöffler and Langenhorst, 1994).

2.2. Biological test systems

Three different kinds of biological test systems were subjected to shock recovery experiments: (i) bacterial endospores (*Bacillus subtilis*), (ii) endolithic microorganisms (*Chroococcidiopsis*), and (iii) epilithic lichens (*Xanthoria elegans*).

2.2.1. Bacterial Endospores. Spores of the gram-positive genus *Bacillus,* a rod-shaped, spore-forming bacteria and a member of the division *Firmicutes* (kingdom *Bacteria*) were used. *Bacillus subtilis* strain TKJ6312 (deficient in the synthesis of the amino acid histidine, methionine, and leucine) was kindly provided by N. Munakata from the National Cancer Center Research Institute, Tokyo, Japan. The deficiency markers allowed for the discrimination of the test organisms against possible contaminations by a marker test as described in Horneck *et al.* (2001b).

Spores were obtained by cultivation under vigorous aeration in Schaeffer sporulation medium, which contained 16.0 g Difco-nutrient broth (BD Diagnostics, Sparks, MD, USA), 2.0 g KCl and 0.7 g $MgSO_4 \times 7\ H_2O$ per liter (Schaeffer *et al*., 1965), for 4 days at 37°C until a sporulation frequency of >90% had been reached, as judged by phase-contrast microscopy. Spores were harvested by centrifugation (10,000 × *g*, 20 min, 4°C) and treated with $MgSO_4$ (2.5 μg/ml), lysozyme (200 μg/ml), and DNAse I (2 μg/ml) for 30 min at 37°C to destroy the residual vegetative cells. The enzymes were inactivated by heating for 10 min at 80°C. After repeated centrifugation and washing in distilled water, the purified spores (about 10^{10} spores/ml) were stored in aqueous suspension at 4°C. Standard microbiological methods for cleaning and sterilizing the tools, gabbro discs, and media used were applied.

2.2.2. Endolithic Cyanobacteria. Chroococcidiopsis [order *Pleurocapsales* (Rippka *et al*., 1979), order *Chroococcales* (Komárek and Anagnostidis, 1998)] strain 029 (isolated from endolithic growth in Nubian sandstone in the Negev Desert) was obtained from the Culture Collection of Microorganisms from Extreme Environments (CCMEE) at the University of Rome, Tor Vergata. The organism was grown in BG-11 medium (Rippka *et al.*, 1979) for 1 month. Then 0.2 ml of the culture at a cell density of 0.5 Absorbance Units at 750 nm (1 cm light path) were plated onto 2% BG-11 agar plates. All cultures and plates were grown under an 18:6 h light/dark period, a light intensity of 50 μmol/m^2/s, and a temperature of 29°C. After 3 months, cells were aseptically harvested from the plates and homogeneously suspended in 4 ml of sterile H_2O to a final absorbance value of 0.5 at 750 nm (1 cm light path) for further use in the experiment.

2.2.3. Epilithic Lichens. Taxonomically, lichens are classified as fungi and represent a 600-million-year-old symbiosis of a fungus and an alga (Yuan *et al.*, 2005). In our experiment, the lichen *Xanthoria elegans* was selected for the performed experiments as one representative of such a eukaryotic and symbiotic system where the alga *Trebouxia* as photosynthetic organism (photobiont) is bound into symbiosis with a fungus (mycobiont). *Xanthoria elegans* (Link) Th.Fr. was collected together with its natural rock substrate (gneiss and dolomite as calciferous rock) near the Sanetsch Glacier (Wallis, Switzerland, GPS: N46°21.799′, E007°17.844′) for experiments at 41.5–50 GPa, or at the Seiser Alm (South Tyrol, Italy: N46°54′, E11°62′) for the experiments at 5–30 GPa. All samples were stored in a frozen state at −20°C until used in the experiments.

2.3. Selection and properties of host rock

About 70% of the known martian meteorites are coarse-grained basalts with a texture not unlike terrestrial gabbros (*e.g.*, Meyer, 2006). Therefore, 2 large samples of terrestrial gabbro from the Bushveld Complex in South Africa were selected as host rock for the biological test systems. Serving as representatives of one of the most typical upper crustal rocks of Mars, they also satisfy the requirements imposed by the shock experiments and the subsequent analytical procedures. This rock material is free of weathering products and contains relatively coarse-grained plagioclase, which can be separated relatively easily from the shocked samples for the determination of shock effects in individual grains. This allows

for a statistically valuable distribution of the shock pressure throughout the shocked sample. The modal compositions of the 2 Bushveld gabbro samples are slightly different. The plagioclase content (given in volume percent) ranges from 61–69%, whereas the content of ortho- and clinopyroxene varies from 21–27%. Minor constituents are about 7% olivine (type 1), <10% quartz (type 2), and ore minerals. The plagioclase content is higher than that of martian basaltic meteorites, which have a plagioclase content in the range of 25–50 vol % (Meyer, 2006). In the terrestrial sample, the plagioclase has the composition of labradorite to bytownite, *i.e.*, the anorthite (An) content ranges from about 56–78 mol % in one type of gabbro and 65–72 mol % in the other type, with an average in the labradorite range ($An_{50–70}$). The composition of orthopyroxene is that of hypersthene with about $En_{62}Fs_{35}Wo_3$ (En = enstatite, Fs = ferrosilite, Wo = wollastonite). Clinopyroxene is an augite with about $En_{40}Fs_{15}Wo_{45}$, and olivine has a forsterite content of 63–66 mol %. The grain size of plagioclase and of the pyroxenes ranges from several 100 μm up to 7 mm. Both types of gabbro samples display a cumulate texture similar to that found in many martian meteorites.

2.4. Sample preparation for shock recovery experiments

Cylindrical cores were taken from the gabbro samples and cut into thin discs with a diameter of 15 mm. The raw discs were shaped to a thickness of 0.5 mm and polished with diamond paste (1 μm grain size) on both sides. For shock recovery experiments, the microbial samples were sandwiched between 2 discs (Fig. 4). The thickness of the microbial layer ranged from a few μm (1–7 μm), in the case of bacterial spores and cyanobacteria, to about 50 μm for the lichen samples.

B. subtilis spores (5×10^7 spores in 100 μl) were spread uniformly on the polished surface of the gabbro disc and dried in air at room temperature. The spores formed a monolayer of about 1–2 μm in thickness with an average density of 1.3 g/cm^3 (Berlin *et al.*, 1963; Baltschukat and Horneck, 1991). The spore-loaded disc was covered with another spore-free disc, and the sandwich was mounted at the sample site of the ARMCO-iron container (Fig. 3). It was stored in the closed container at room temperature until the experiment was carried out.

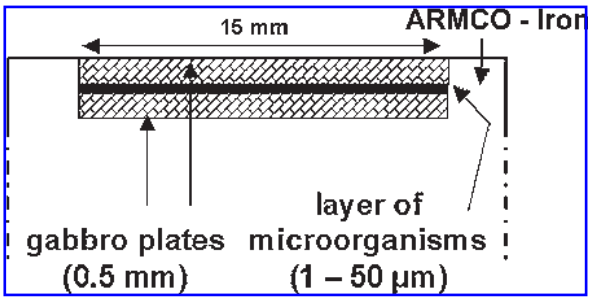

FIG. 4. Sketch of the microbe-loaded sample with a diameter of 15 mm.

An aliquot of *Chroococcidiopsis* cells (200 μl) of 0.5 Absorbance Units at 750 nm (1 cm light path) was dispensed onto the polished surface of the rock disc. The thickness of the microbe layer varied from 2.5 to about 7 μm with a density in the range of 1 g/cm^3. The rock slice with the cell layer was placed into a Petri dish and allowed to dry slowly in darkness at 21°C. Then it was treated similarly to the disc sandwich loaded with *B. subtilis* spores.

Several slices (about 50 μm in diameter and height) of the lichen *Xanthoria elegans* composed of lichen thalli and fruiting bodies were deposited on the gabbro disc. They were very closely packed to keep interstitial space at a minimum. After drying, the lichen-loaded disc was covered with a second gabbro disc (simulating an artificial endolithic lichen sample) and mounted into the ARMCO-iron sample container.

2.5. Performance of shock experiments and recovery of shocked rock and biological samples

The microbiological samples within the double disc of gabbro were emplaced in the 1 mm deep borehole on top of the cylindrical inner sample container as shown in Fig. 3. For each experiment, the dimensions of the ARMCO-iron container and of the flyer plate, as well as the type of high explosive, were chosen according to the values given in Table 1 to achieve the desired shock pressure. These "nominal" shock pressures, which have an accuracy of about ±3%, were chosen for each of the 3 types of microorganisms to be at the following levels: 5, 10, 15, 20, 30, 41.5, and 50 GPa (Table 1). All experiments were performed at room temperature. A control sample identical to the one that was shock loaded was prepared for all experimental runs and stored in the laboratory

TABLE 1. PARAMETERS OF THE HIGH-EXPLOSIVE DEVICE AND OF THE AIR PRESSURE GUN FOR DIFFERENT SHOCK PRESSURES (COMPARE FIGURE 3)

Pressure P *(GPa)*	*Cover plate* D *(mm)*	*Flyer plate* d *(mm)*	*High explosive [∅ (mm)]*	*Velocity of flyer plate* v *(km/s)*	*Pulse length (μs)*
4.6	3	4	Air-pressure gun	0.228	1.34
10	20	4	TNT (64)	1.549	1.35
15	10	4	TNT (64)	1.549	0.88
20	17	4	Holtex (64)	1.888	0.59
30	11	4	Holtex (64)	1.888	0.32
41.5	9.5	3	Composition B (64)	1.992	0.08
50	10	4	OWC (80)	2.540	0.17

for later evaluation in parallel with the shocked sample.

The air gun and the high-explosive devices, as defined in Table 1, were ignited in a special shelter facility of the Ernst-Mach-Institute. Immediately after the shot, the inner sample container (ARMCO iron), which usually showed some plastic deformation, was recovered from the broken-up outer steel container (Fig. 5a). The containers shocked to pressures higher than 10 GPa were quenched in cold water (0°C) a few minutes after the explosion. They were then taken to the machine shop, and the lower part of the iron container was carefully machined down until the inner cylindrical part with the sample could be retrieved. The container was continuously cooled during this grinding operation. In all experiments, the microbe-loaded gabbro sample disc could be recovered completely (Fig. 5b). Each recovered sample was stored separately at 4°C and distributed to the different laboratories for further analysis.

2.6. Analyses

2.6.1. Mineralogical and Petrographic Analyses. The texture and shock effects of the shocked gabbro were studied by optical microscopy, micro-Raman spectroscopy, and microchemical analyses in polished thin sections made from selected parts of the sample discs. The 2 discs of each sandwich were analyzed separately. The actual shock pressure experienced by the constituent minerals of the gabbro samples was estimated qualitatively on the basis of characteristic shock effects in plagioclase, pyroxene, and olivine (see reviews in Stöffler, 1984; Stöffler *et al.*, 1986, 1991). The shock pressures recorded by plagioclase were determined quantitatively on the basis of the refractive indices (RIs) of this mineral. Their values

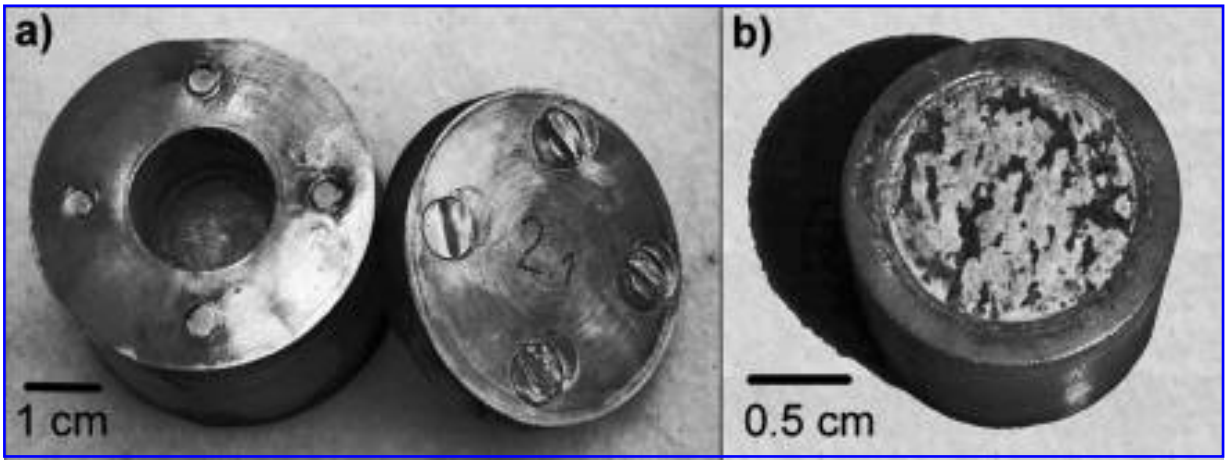

FIG. 5. (a) Sample container (ARMCO iron) and (b) sample holder with gabbro disc (15 mm diameter) after the shock recovery experiment (compare Fig. 3).

have been calibrated previously by shock recovery experiments on plagioclase and plagioclase-bearing rocks (Stöffler *et al.,* 1986). However, this method is only applicable for plagioclase shocked to pressures above about 15–20 GPa.

After the optical inspection, the plagioclase grains were investigated in thin sections *in situ* by micro-Raman spectroscopy with a notch filter–based Dilor LabRam and a HeNe laser of 632 nm wavelength. The sample excitation and Raman scatter collection was performed using a 100× optical lens on the Raman microscope. Energy of 3 mW was transferred to the sample surface with a spot size of 2.5 μm. The Raman spectra were collected from 300–1200 cm^{-1}. The final spectra represent the accumulation of 20 single spectra, each of which were recorded with a collecting time of 10 s. Backgrounds of the final spectra were graphically reduced by linearly interpolating over discrete frequency ranges. Gauss-Lorenz fitting was used to deconvolute the recorded spectra.

To detect a possible spatial variation of the intensity of shock effects, the shocked gabbro discs of the 20, 30, and 41.5 GPa experiments were subdivided into 3 parts that represented different radial distances from the center of the disc. From each area, several milligrams were crushed and plagioclase grains of 50–300 μm were hand picked under the microscope. Their RI was determined by the so called "λ-T" immersion method (*e.g.,* Kleber, 1970) with the use of a special device developed at the Berlin Institute of Mineralogy (Fritz *et al.*, 2002, 2005). Afterward, polished thin sections of the grains were produced for a quantitative determination of chemical composition (An-content) by a JEOL JXA-8800L electron microprobe operating at 15 kV with a beam current of 10 nA and a beam size of 10 μm. Suitable mineral standards, including plagioclase, chromium augite, and anorthoclase (all certified by the United States National Museum as reference samples for electron microprobe analysis) were applied. Finally, the RIs and the chemical composition of the individual plagioclase grains were plotted in a calibration diagram, which allowed us to deduce the shock pressure recorded by the analyzed plagioclase grains (Stöffler *et al.,* 1986).

2.6.2. Calculation of Shock and Post-Shock Temperature. Shock compression is a non-isentropic process, by which the shocked material is heated during compression to a certain temperature, *i.e.*, the shock temperature. Subsequent adiabatic decompression leaves the shocked material at an elevated temperature, *i.e.*, the post-shock temperature. Both temperatures increase with increasing shock pressure. The amount of "waste heat" deposited in any material upon shock compression is determined by the thermodynamics of discontinuous non-isentropic shock loading and subsequent adiabatic unloading. Accurate values for the shock and post-shock temperatures of the inner iron container and the gabbro samples were calculated using experimentally determined equations of the state of the 2 materials. The calculations of shock and post-shock temperatures (Artemieva and Ivanov, 2004; Fritz *et al.*, 2005) are based on experimental equations of state, which shows a linear correlation of particle velocity u_p and shock wave velocity U: $U = c + s \times u_p$, where c and s are experimentally determined constants. The values of the constants c and s are 3.75 and 1.66 for $\text{iron}_{(<270\ \text{GPa})}$ (McQueen and Marsh, 1960), and 5.54 and 0.26 for $\text{gabbro}_{(<32\ \text{GPa})}$ (Trunin *et al.,* 2001), respectively. With regard to the determination of the actual post-shock temperatures achieved in the microbe-loaded gabbro samples, it must be taken into account that the iron container is subjected to the final peak shock pressure directly by the first shock wave P (Appendix), whereas the gabbro acquires the final peak shock pressure via a sequence of shock reflections. Thus, temperatures for the iron container are calculated for the nominal shock pressure. In contrast, only the first shock wave, which induces a relatively low pressure in the gabbro, dominates the amount of waste heat deposited in the shocked gabbro (*e.g.,* DeCarli *et al*., 2002). The contributions of the subsequent reflected shock waves can be neglected in the calculation of the post-shock temperatures achieved in gabbro.

2.6.3. Biological Analyses. 2.6.3.1. B. subtilis *endospores.* After exposure to different shock pressure scenarios, spores were stripped from the gabbro discs by the PVA technique (Baltschukat and Horneck, 1991; Horneck *et al*., 2001a), which resulted in >95% recovery of the spores. Survival of the spores was determined from their ability to form colonies. Spore suspensions in appropriate dilutions were plated on nutrient broth agar plates. Colonies were scored after 18 h of incubation at 37°C. Surviving fractions were determined as N/N_0 where N was the number of

colony-forming units of the treated samples and N_0 that of the untreated control. Mean values and standard errors were calculated for each sample from up to 6 replicate plates. A marker test of the colonies from the experiment samples (Horneck *et al.*, 2001b) was performed to check for possible contamination of the samples.

2.6.3.2. Chroococcidiopsis *cells (vegetative).* Following the shock experiment, the cells were resuspended in BG11 directly from the rock material. A similar procedure was followed for the unshocked control.

Three following methods were used to assess viability:

(1) Direct colony counts. This was considered the most robust method to determine cell survival. Cells were plated onto BG-11 agar plates at 1, 10, and 100 × dilutions, with four plates per dilution. Plates were incubated as described above, and after 2 months the number of colony-forming units on the control and impact-shock plates were enumerated and the loss of viability calculated.
(2) Localization of nucleic acid to the interior of the cell was assessed using the DNA-binding dye DAPI (4′,6-diamidino-2-phenylindole dihydrochloride). Rehydrated cells (10 μl) were added to 10 μl of DAPI (Sigma Chemicals, Dorset, UK) on a glass slide. DAPI was added at a concentration of 1 μg/ml, and cells were incubated at room temperature for 15 min in darkness. For DAPI visualization, cells were imaged using a Leica DMRP microscope equipped for epifluorscence with a Leica A cube (band pass 340–380 nm), and cells were observed at an emission wavelength of >425 nm.
(3) The fluorescence of the light-harvesting pigments (phycobilisomes) was determined as a measure of the degradation of the photosynthetic apparatus at the Multi-Imaging Center, University of Cambridge. Rehydrated cells were examined under a Leica TCS-SP-MP confocal laser microscope (Leica Microsystems, Heidelberg, Germany). Cells were irradiated with a 568 nm laser, and fluorescence at wavelengths greater than 590 nm was measured. Ten fields of view were chosen, and by way of the Leica LCS software, fluorescence was measured across the field of view along a transect between 10 and 30 μm in length. Fluorescence was then expressed in units per μm. Fluorescence was compared with the control cells.

2.6.3.3. Xanthoria elegans *lichen.* To determine the vitality of the lichen tissue after the shock experiments, the samples were stained with live/dead dye FUN I (Molecular Probes / Invitrogen) and analyzed by use of a confocal laser scanning microscope (CLSM Leica TCS NT). FUN I marks only vital and metabolically active cells with production of fluorescent intravacuolar structures due to the cell activity. The intravacuolar structures were stained by FUN I with a red fluorescent color and the surrounding cytoplasm by an intense green to yellow fluorescence. Depending on physiological activity of the cells, the green color changes rapidly into red fluorescence. Dead cells show a diffuse, green-yellow fluorescence and do not change their color. For excitation, ArKr and HeNe lasers were selected with excitation filters 488/568/647 nm and 488/568/633 nm, both with a defined transmission of 50%. The images were analyzed using Leica TCS-NT/Confocal Systems Software. Channel-imaging was correlated with contour images and overlay images to improve recognition of visual damage, which reflects the vitality of the lichen tissue. Channel-imaging emission filters in 3 different fluorescence ranges were applied. Band pass filters at 548 nm, 559 nm, and 506 nm were used for green, red, and blue fluorescence, respectively. From the

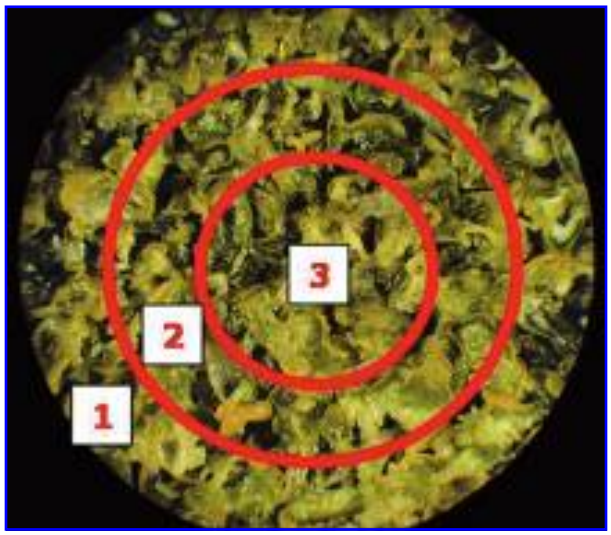

FIG. 6. Gabbro disc loaded with lichen tissue and subdivided in three areas: 3, central area with a radius r of 0.25 cm; 2, middle ring from r = 0.25 to 0.50 cm; 1, outer ring at r > 0.50 cm.

quantitative data on the vitality of the shocked samples that were stained by live/dead-dye, FUN I mean values were determined, which indicated the deviation of the ratio of vital tissue t_v to the whole lichen thallus t_o. Vital and nonvital cells of both bionts, the photobiont and mycobiont, in the lichen tissue were quantified by the cell-counting program of Image Tool and by CLSM fluorescence intensity diagram analysis (de Vera *et al.*, 2003).

To determine whether the vitality of the shocked lichen tissue depends on its location on the gabbro disc during the shock wave exposure, the lichen-loaded gabbro discs were subdivided into three areas: a central area and 2 surrounding rings (Fig. 6). Lichen tissue from each area was analyzed separately by CLSM as described above.

3. RESULTS

3.1. Physical state of recovered samples

The optical appearance of the shocked gabbro changed due to shock loading (Fig. 7). Plagioclase lost its luster and transparency in the experiments up to 20 GPa due to intense fracturing. Because of the transformation of plagioclase to diaplectic glass (maskelynite) or normal glass at higher shock pressures, it became lustrous and transparent at shock pressures between 30 and 50 GPa.

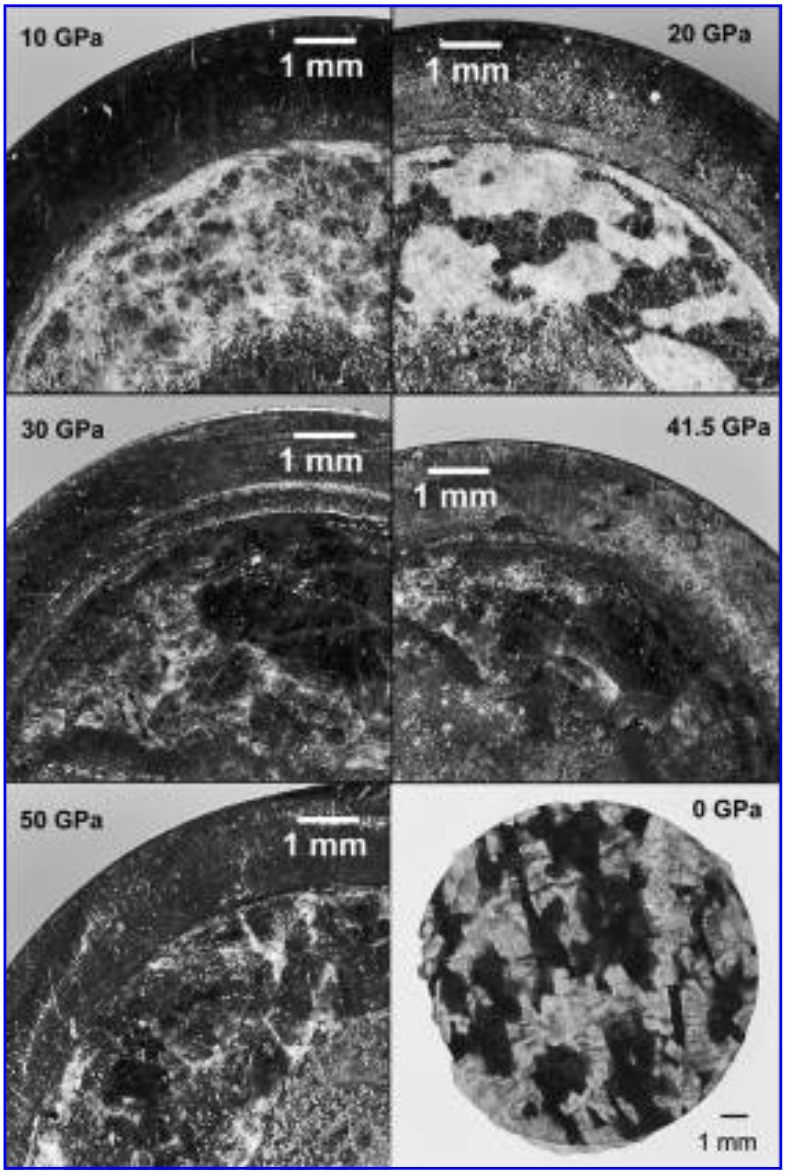

FIG. 7. Photograph of microbe-loaded gabbro discs (still emplaced in the iron sample holder) that was shocked at 5 different pressures, as well as a sample disc of unshocked gabbro (diameter: 15 mm), collected from Bushveld Complex in South Africa for the experiments: dark grains, pyroxene and olivine; white grains, plagioclase.

Pyroxene lost its brownish color and brightness with increasing shock pressures. The original igneous texture of the gabbro samples did not substantially change due to the shock compression. Even at pressures of 41.5 and 50 GPa, the original rock texture was well preserved.

The shock compression of the samples resulted in different degrees of conservation of the discs as a whole, depending on the shock pressure. At low shock pressures (5–15 GPa), the gabbro discs were recovered in a somewhat friable state. Therefore, it was not possible to separate the samples into an inner, middle, and outer part. The 20–50 GPa experiments left the gabbro discs in a coherent state, which is, in part, due to shock-induced transformations of the constituent minerals (*e.g.*, transformation of plagioclase into diaplectic glass) and the shock-induced melting of iron from the container at the outer margins of the gabbro discs. In these cases, the exact position of extracted samples was recorded. However, no mineral separation of the outermost zone of the lower gabbro discs was made because of firm adherence of the outer edge of the lower disc onto the ARMCO-iron cylinder.

3.2. Shock pressure and temperature conditions

3.2.1 Calculated Shock Pressures and Pressure Pulse Durations. The final peak pressure in the gabbro samples was achieved by applying the shock reverberation technique. By changing the parameters D and d, seven different peak pressure levels were produced. The duration of the peak pressure in the gabbro sample decreased with increasing pressure from about 1.35 μs at 5–10 GPa to about 0.1 μs at 50 GPa (Table 1)

These "nominal" shock pressures hold for the gabbro host rock. For the microbe-loaded gabbro sandwiches, the shock waves get somewhat "dis-

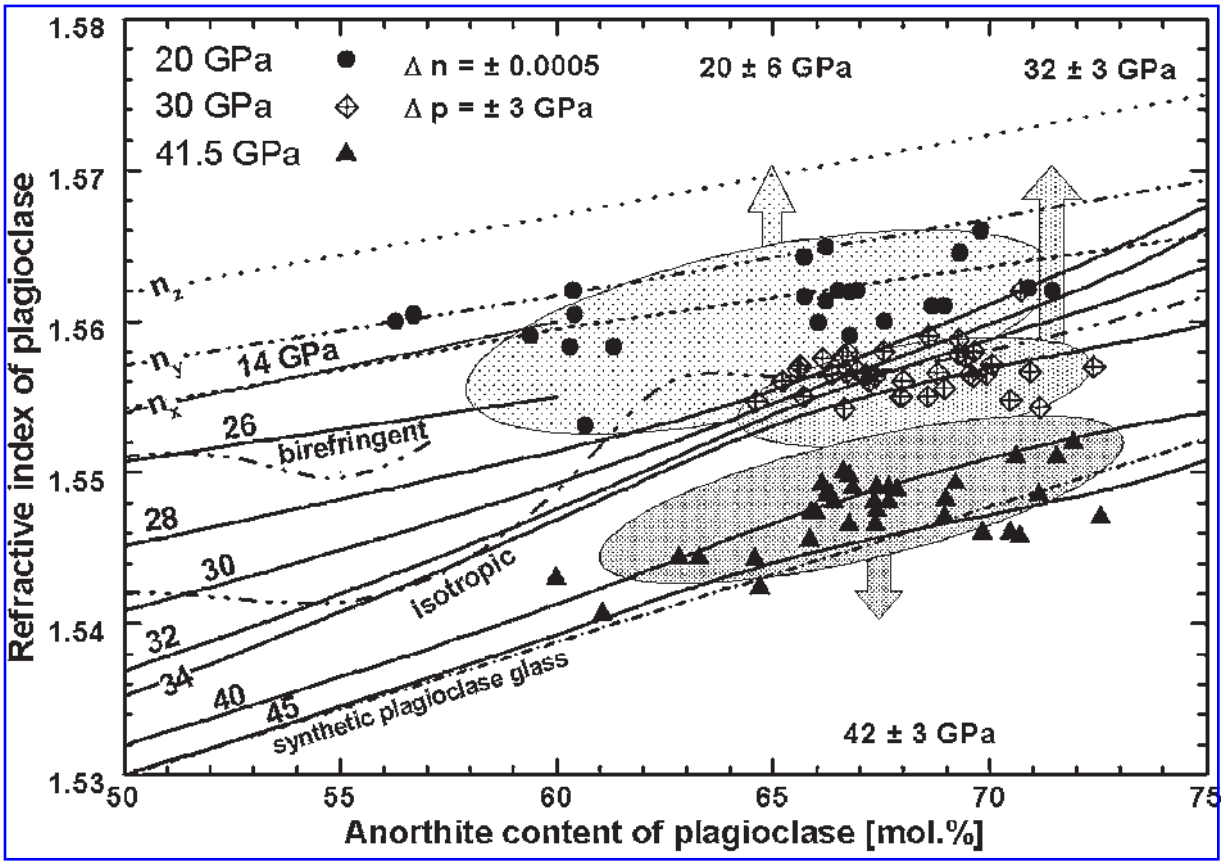

FIG. 8. Refractive indices (RIs) of plagioclase extracted from experimentally shocked microbe-loaded gabbro samples as a function of their chemical composition (An content) for the three shock experiments with nominal pressures of 20, 30, and 41.5 GPa. Dotted lines, RI n_x, n_y, n_z for unshocked plagioclase; solid lines, experimentally determined RI for plagioclase shocked to variable peak pressures (numbers in GPa); dashed-dotted lines, transitions from crystalline to partially isotropic and to completely isotropic shocked plagioclase; dashed line, RI of synthetic plagioclase glass (quenched melt); all calibration data from Stöffler *et al.* (1986).

turbed" due to the lower shock impedance of the thin layer of microorganisms (1–50 μm, depending on the organisms used). A numerical computer code calculation for different thicknesses (7–50 μm) of a water layer substituting for a layer of microorganisms shows that deviations from the final peak shock pressure in the microbial layer were very small, *i.e.*, less than 5% of the nominal peak pressure, and therefore appear to be negligible.

3.2.2. Shock Pressures Determined from Microscopic Analysis and Refractive Index Measurements of Plagioclase. The results of the RI measurements of plagioclase grains are presented in Fig. 8, in which the An content of plagioclase [end members are albite (Ab) = $NaAlSi_3O_8$ and anorthite (An) = $CaAl_2Si_2O_8$] are plotted against the RI (glass) or RIs (crystals). In this diagram, the main refractive indices n_x, n_y, and n_z of plagioclase crystals (upper 3 dashed lines) and of synthetic plagioclase glass (lower straight dashed line) are shown for the 50–80 mol % An range. In addition, shock pressure isobars for shocked plagioclase of variable An content were taken from Stöffler *et al.* (1986) (solid lines and dashed-dotted lines). Depending on composition, the optically birefringent crystals transform into partially isotropic plagioclase and totally isotropic phases (called diaplectic glass or maskelynite) at pressures above about 15 GPa and from 26–34 GPa, respectively. Because plagioclase is shock-fused above about 45 GPa and forms normal glass with RIs identical to synthetic glass, only data from the 20, 30, and 41.5 GPa shots are plotted.

The RI data of plagioclase extracted at different radial distances from the center of the shocked gabbro discs did not show any correlation between the shock pressure and the positions of the extracted samples within the gabbro discs. This means that, within the resolution of the shock pressure indicators, the complete discs were homogeneously shocked. For this reason, the shock pressures measured in different grains were averaged for each shock experiment. The scatter of data in Fig. 8 is mainly due to the (natural) variation of the An content of plagioclase in the gabbro samples (about $An_{55–75}$). Because of the low sensitivity of the RI of plagioclase against shock compression at 20 GPa, the plagioclase grains of this experiment exhibited refractive indices, which were only somewhat lower than n_y with a rather large scatter, indicating actual pressure values between 14 GPa and 26 GPa with a large error of ±6 GPa. The average shock pressures recorded by plagioclase in the 20, 30, and 41.5 GPa experiments were 20 ± 6, 32 ± 3, and 42 ± 3 GPa, respectively. These results show a satisfactory agreement between the nominal shock pressures and the measured shock pressures.

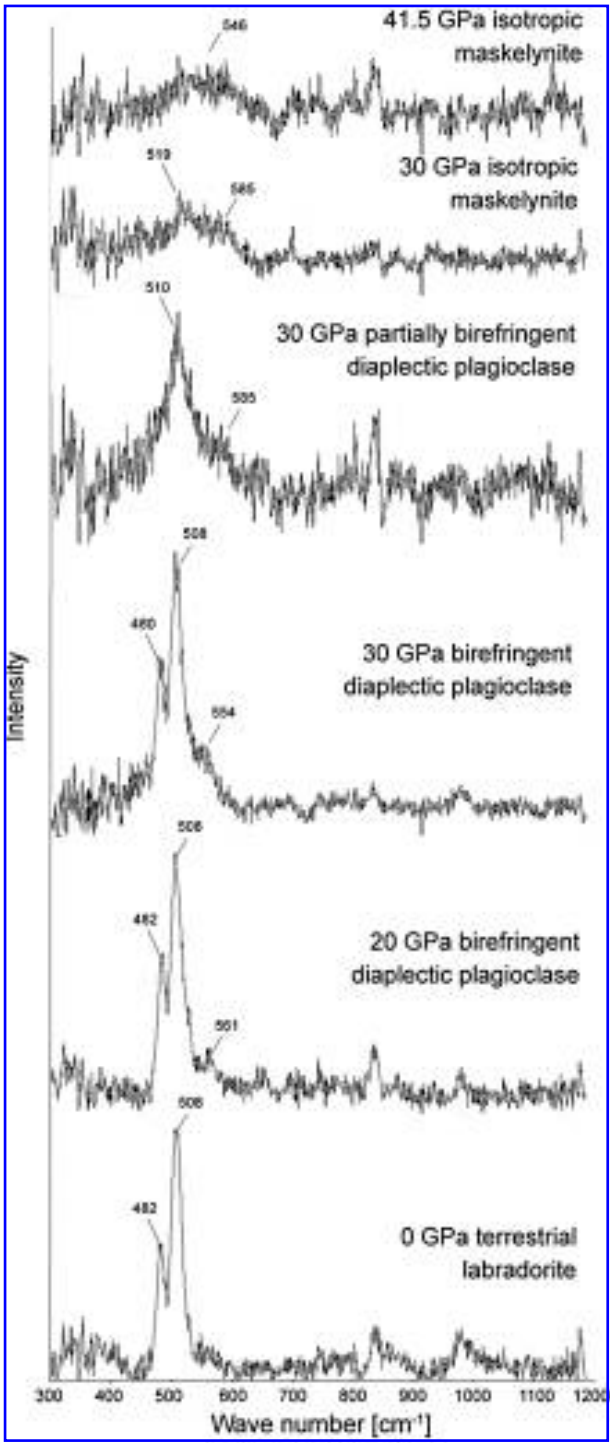

FIG. 9. Raman spectra of unshocked and shocked gabbro samples for 20, 30, and 41.5 GPa.

The actual peak shock pressures achieved in the samples from the remaining experiments at the nominal pressures of 5, 10, 15, and 50 GPa could only be checked qualitatively on the basis of various shock effects in plagioclase, pyroxene, and olivine for which pressure calibration data also exist (*e.g.*, Stöffler, 1984; Stöffler *et al.*, 1991).

The intensity of shock metamorphism of gabbro achieved in the experiments at 5, 10, and 15 GPa were documented by mechanical twinning and undulatory extinction in pyroxene, undulatory extinction in olivine and plagioclase, and by the lack of mosaicism in pyroxene and olivine, and the absence of planar fractures in olivine. These observations indicate clearly a minimum pressure of 5 GPa and a maximum pressure in the range between 15 and 20 GPa, but they reveal no information about the exact shock pressure (Stöffler *et al.*, 1991).

Samples from the 20 GPa experiments showed birefringent (diaplectic) plagioclases with mosaicism and numerous fractures. These observations were confirmed by Raman spectroscopy (Fig. 9) that indicated exclusively birefringent (diaplectic) plagioclase, which implies a maximum shock pressure of 26 GPa (Stöffler *et al.*, 1986). However, some melt veins and melt pockets, mainly at fractures, inferred local shock pressures and temperature excursion. Pyroxene displays strong undulatory extinction in transition to weak mosaicism. Olivine displays weak mosaicism and planar fractures. The observed effects are compatible with a shock pressure of about 20 GPa.

Plagioclase from the 30 GPa experiments was partially to completely isotropic. The Raman spectra also indicated the existence of remaining small areas of birefringent plagioclase (Fig. 9). Weak to strong mosaicism in olivine was observed in these samples. The pyroxenes showed a transition from undulatory extinction to mosaicism. Planar deformation features were developed in clinopyroxene and planar microstructures in olivine and orthopyroxene. These observations are in perfect agreement with a shock pressure range from about 28–30 GPa, as indicated by the calibration data for plagioclase of An_{55}-An_{75} composition (Fig. 11 in Stöffler *et al.*, 1986).

In the 41.5 GPa experiments, plagioclase was completely converted to diaplectic glass (maskelynite). This agrees with the data from Raman spectroscopy (Fig. 9). Rarely, maskelynite showed flow structures and vesicles and sometimes thin edges of recrystallized plagioclase. In a few cases only, olivine showed recrystallization, mainly in melt pockets and melt veins. The absence of brown staining of olivine and the rare vesiculation in plagioclase glass indicates a pressure of less than about 45 GPa (Reimold and Stöffler, 1978; Stöffler *et al.*, 1986). On the other hand, strong mosaicism, irregular and planar fractures,

TABLE 2. CALCULATED SHOCK AND POST-SHOCK TEMPERATURE INCREASES ACHIEVED IN THE IRON CONTAINER AND THE MICROBE-LOADED GABBRO SAMPLES AS A FUNCTION OF PEAK SHOCK PRESSURE

P *nominal gabbro (GPa)*	P *gabbro (GPa)*	ΔT_2 *shock in gabbro (K)*	ΔT_3 *post-shock in gabbro (K)*	ΔT_3 *post-shock in iron (K)*	ΔT_4 *final post-shock in gabbro (K)*[a]
Reverberation[b]	*First wave*			*Reverberation*[b]	
5		<1	<1	1	<1
10	6.6	1	1	8	7
15	9.3	3	2	22	20
20	12.2	7	6	45	39
30	17.4	23	17	126	109
41.5	22.7	53	35	244	210
50	26.8	99	56	352	304

P = pressure, ΔT = temperature increase relative to pre-shock ambient temperature induced by a given shock pressure.

[a]After heat exchange with the steel container.

[b]*P* or *T* achieved after multiple shock-wave reverberations in gabbro; the surrounding iron container is directly shocked to the final pressure.

TABLE 3. RESULTS OF COMPUTER CODE CALCULATIONS OF THE SHOCK TEMPERATURE INCREASE ΔT AND DURATION IN A WATER LAYER (SUBSTITUTE FOR THE MICROBIAL LAYER) OF 7 μm AND 50 μm THICKNESS AS A FUNCTION OF PEAK SHOCK PRESSURE IN THE HOST GABBRO

Shock pressure (GPa)	*Shock temperature ΔT_2 in host rock (K)*	*Shock temperature ΔT_1 in water layer (K)*	*Duration of shock temperature in water (μs)*
	gabbro 7 μm		
10	1	80	<1.3*
30	23	450	<0.3*
	gabbro 50 μm		
10	1	80	<1.3*
30	230	420	<0.3*
40	350	890	<0.3*
	dunite 50 μm		
18	2	210	0.4
40	250	930	0.4

For comparison, data for a 50 μm layer in a dunite host rock are given (B.A. Ivanov, personal communication); compare Fig. 18.
*Exact values cannot be obtained from the applied method of calculation.

and planar deformation features in olivine and pyroxene point to shock pressures of more than 35 GPa (Bischoff and Stöffler, 1992).

Vesiculated plagioclase melt was frequently observed in the 50 GPa samples. For this transformation, shock pressures higher than 45 GPa are needed (Stöffler and Hornemann, 1972; Stöffler *et al.*, 1986). Olivine displayed brown staining. This effect has been observed in the pressure range from 44–56 GPa (Reimold and Stöffler, 1978). Based on these observations, a shock pressure between 45 and 55 GPa was deduced.

3.2.3. Calculated Shock and Post-Shock Temperatures in Host Rock and Microbial Layer. The calculated shock and post-shock temperatures are presented in Table 2. It should be noted that, in contrast to a single-shock compression, the post-shock temperatures in the gabbro samples were distinctly lower than those achieved after pressure release in the iron container because of the reverberation technique and the different Hugoniot parameters for gabbro and iron. It is only the first wave entering the gabbro that really heats the sample.

As in the case of the peak shock pressures, the actual temperatures achieved in the thin microbial layer required a special consideration in the course of the temperature calculations. The numerical calculations regarding the effects of a thin water layer (substituted for the microbial layer because of the lack of Hugoniot data for microorganisms) on the shock temperature show that there is a very strong positive excursion of the shock temperature, though for a very short period of time (Table 3). The compression of the few μm thick low-density water layer leads to an irreversible and significant increase in local temperature due to the very low shock impedance of water compared to gabbro. It

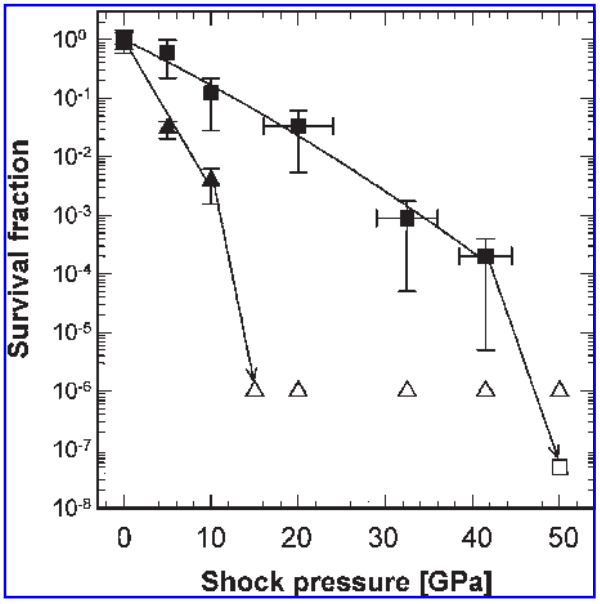

FIG. 10. Survival rate of spores of *B. subtilis* TKJ 6312 (squares) and cells of *Chroococcidiopsis* sp. (triangles), encased in gabbro plates plotted against the shock pressure to which they were exposed in the shock recovery experiments. Data points are mean values and error bars give 1 σ deviation. The curves were calculated using SigmaPlot 9.0 software. The open symbols indicate survival below the threshold of detection.

is important to note that the high-pressure regime of the phase diagram of water reveals that water would be transformed to ice VII under the pressure conditions achieved in our experiments (Stewart and Ahrens, 2005).

3.3. *Effects of shock pressures on the biological test samples*

3.3.1. B. subtilis *Spores.* Survival of shocked spores of *B. subtilis* decreased exponentially with increasing shock pressure (Fig. 10). The survival curves were calculated using SigmaPlot 9.0 (Systat Software Inc., San Jose, CA, USA). The regression factor (Pearson correlation coefficient) of a second-order regression amounted to $r = 0.989$. The survival rate was reduced to about 10^{-4} for spores exposed to a shock pressure of 41.5 GPa. At higher shock pressures, such as 50 GPa, survival rates dropped below their threshold of detection at 5×10^{-8}. The genetic marker test proved that all colonies were of strain *B. subtilis* 6312, which demonstrates that the samples were not contaminated.

3.3.2. Chroococcidiopsis *Cells.* Some *Chroococcidiopsis* sp. 029 cells were able to survive shock pressures up to 10 GPa (Fig. 10). The regression factor of the survival curve (first order regression) was $r = 0.977$. At higher pressures, however, there was an abrupt loss of viability. Bright field microscopy revealed that many of the cells had ruptured at 10 GPa, which accounts for the loss of viability at this pressure (Fig. 11). At 30 GPa, there were no intact cells and all were ruptured.

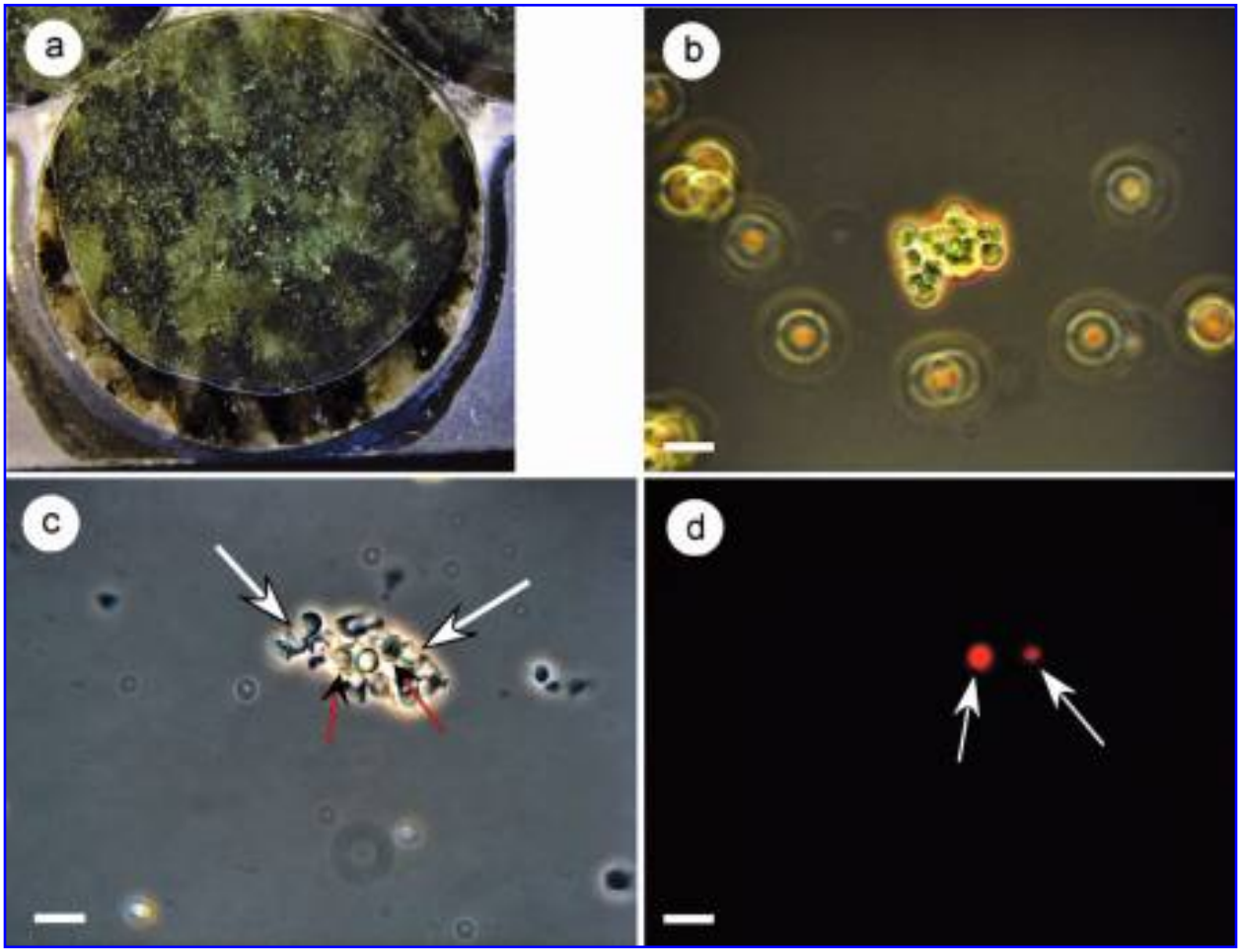

FIG. 11. ***Chroococcidiopsis*** **sp. 029 (a) as thin layer mounted on the gabbro disc, (b) cells in suspension, (c) and (d) after being shocked to 10 GPa.** The white arrows show ruptured cells and loss of cell contents, (d) autofluorescence of the same field of view. Two cells [red-line arrows in (c), white arrows in (d)] still retain autofluorescence, which indicates integrity of cell membranes; the remaining cells have suffered complete loss/destruction of their photosynthetic pigments. [scale bar 10 μm in images (b) to (d)]

Ruptured cells showed neither DAPI fluorescence nor autofluorescence, which indicates that the photosynthetic apparatus had been destroyed or lost from the cells along with nucleic acids and is consistent with bright field observations. Despite the survival of many cells at 10 GPa, autofluorescence was reduced, which suggests that sublethal damage to the photosynthetic apparatus occurred in those cells that were still viable. However, cells with lowered autofluorescence showed DAPI fluorescence, which demonstrates localization of nucleic acids in the center of the cells and is consistent with bright field observations of the maintenance of cell integrity and cell ability to form colonies.

3.3.3. Xanthoria elegans *Thalli.* After evaluation of the CLSM images of shocked lichen samples on the gabbro surface, we determined the active staining index, *i.e.*, the rate of vital to nonvital cells of lichen tissue, by fluorescence analysis and the cell-counting program of Image Tool. Figure 12 shows the active staining index of both the photobiont and the mycobiont as a function of shock pressure. The regression factor for the curves (second order regression) was $r = 0.997$ for the photobiont and $r = 0.976$ for the mycobiont. It should be noted that this vitality test of the lichens indicates the integrity of the membranes as well as the physiological processes of the cells, which is different from the colony counts applied for the 2 other microbial test systems. The dose-effect curve of the mycobiont, which was more resistant than the photobiont, shows a shoulder, and there was no significant inactivation of the mycobiont at shock pressures up to 10 GPa. At 41.5 GPa, the vitality was reduced to 10^{-4}, a value similar to that for the survival of bacterial spores (Fig. 10), whereas no viable photobiont cells were detected at these pressures. At 50 GPa, the highest shock pressure tested, vitality of the mycobiont was reduced to 2×10^{-5}, which is close to the detection threshold of any viable cell. Under these conditions, only a few vital ascospores were detected.

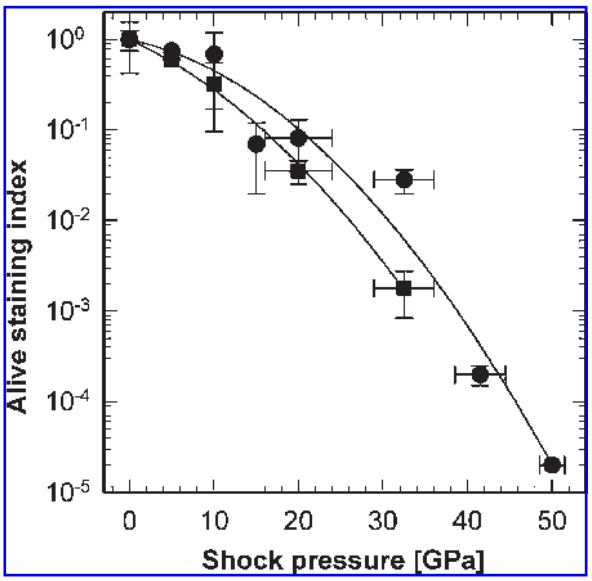

FIG. 12. Vitality of mycobiont hyphae (filled circles) and photobiont cells (filled squares) of *Xanthoria elegans* in shocked lichen tissue as a function of shock pressure. Data points are mean values and error bars give 1 σ deviation. The curves were calculated using SigmaPlot 9.0 software.

The reconstruction of the location of the different lichen thalli on the gabbro discs during the shock pressure treatment (Fig. 6) allowed for correlation of the observed cellular damage with the area on the gabbro disc in addition to the shock pressure level. Figure 13 shows a fruiting body of the non-treated control group. While the thallus is differentiated in an upper cortex with crystallized secondary lichen metabolites, a photobiont layer, and medulla, the fruiting body (Apothecium) is characterized by an upper hymenium layer encrusted with crystallized secondary lichen metabolite parietin, hymenium with paraphysis and spores, hypo-hymenium, photobiont layer, and medulla.

After the shock experiments, these well-ordered structures were less detectable, especially in those thalli that were mounted in the center of the gabbro disc (Fig. 14). While the structure of the lichen thallus remained nearly intact at the margin of the gabbro plate (Ring 1) after shock experiments at 10 GPa, lichens located at the inner parts of the gabbro (Area 3) demonstrated fissures and destroyed thalli arrangements after treatment with the same shock pressure. This gradient from rim to center was less expressed at higher shock pressures (20–30 GPa); however, the degree of damage increased with increasing pressure—the structure of the thalli became more and more destroyed. The fraction of vital photobiont cells decreased dramatically, but some hyphae disrupted from the original thallus arrangement still showed vitality.

After shock experiments at 41.5 and 50 GPa,

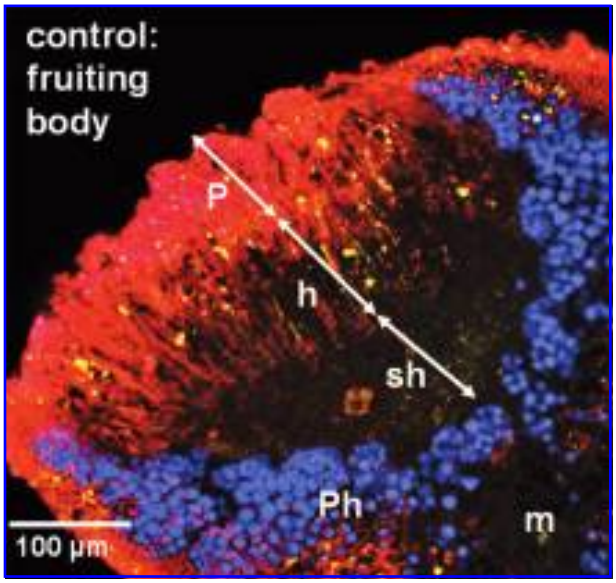

FIG. 13. Lichen thallus of *Xanthoria elegans* with fruiting body of the control group stained with FUN I. h, hymenium; m, medulla; P, Parietin layer; Ph, Photobiont layer; sh, subhymenium.

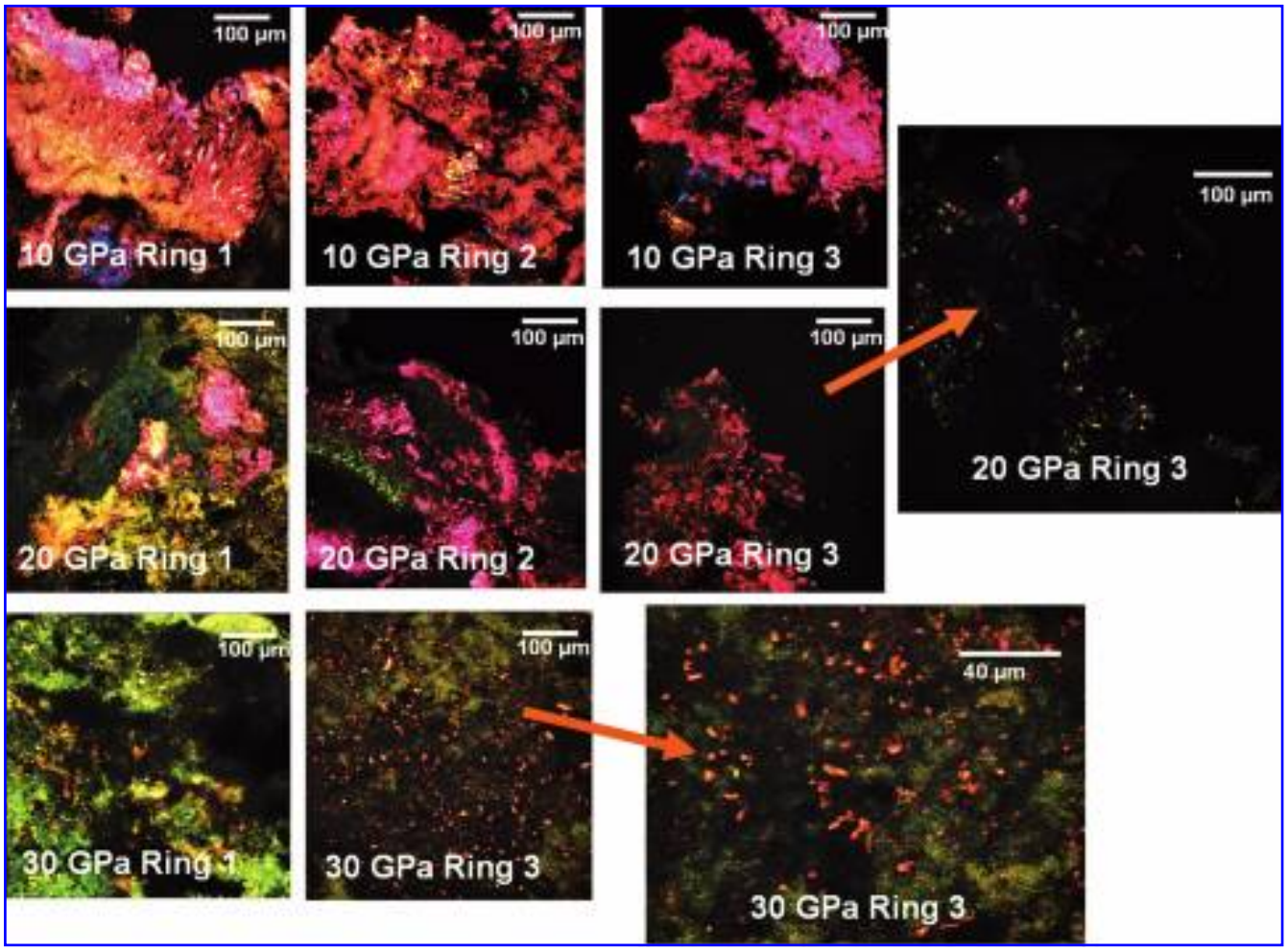

FIG. 14. Thalli and fruiting bodies of *Xanthoria elegans* from different areas of the gabbro disc after shock wave experiments at 10–30 GPa and staining with FUN I (see Fig. 6 for the location of the samples).

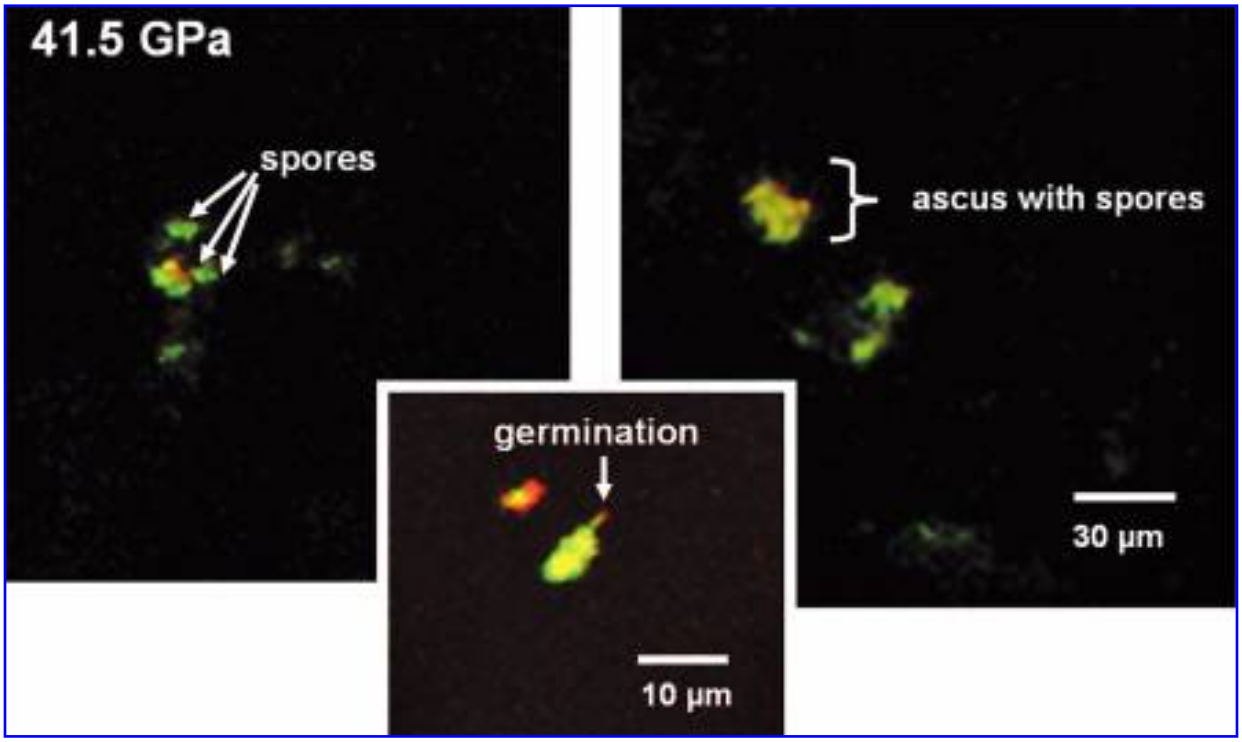

FIG. 15. Only spores and clusters of spores in asci of *Xanthoria elegans* showed vitality after shock experiments at 41.5 GPa, as determined after staining with FUN I.

only the generative part of the lichen, the ascospores, showed vitality (Figs. 15 and 16). Some spores started to germinate after the shock events when exposed to water.

4. DISCUSSION

In this study, we have tackled this question: can endolithic microorganisms survive the severe

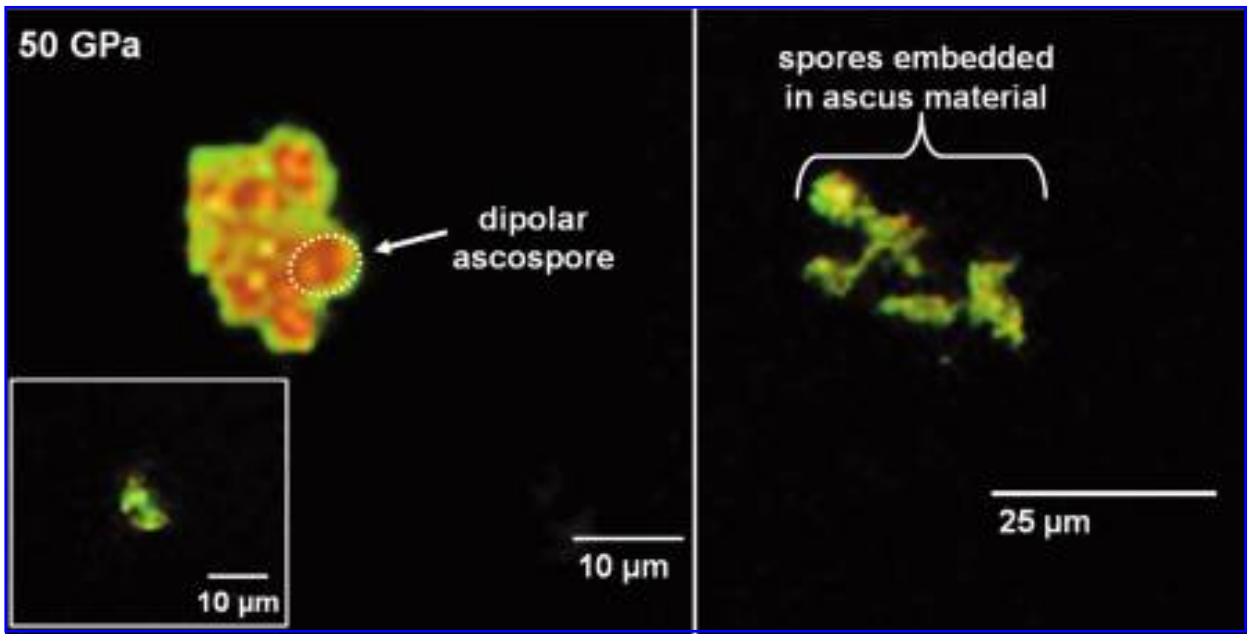

FIG. 16. Dipolar ascospores of *Xanthoria elegans* shocked at 50 GPa stained with FUN I. Storage of physiological metabolites into vacuoles, which are stained red.

conditions of a meteorite impact and ejection event, *e.g.*, from the surface of Mars or another hypothetical inhabited planet of comparable mass? Derived from the conditions recorded in the known martian meteorites, the impact and ejection process involves 3 factors potentially deleterious to life: (i) the shock pressure experienced during the ejection of rocks to escape velocities, which needs to be at least 5 km/s for Mars-like planets; (ii) the acceleration during the ejection process; and (iii) the magnitude and duration of the shock-induced temperature increase. Jerks and accelerations of rock fragments, comparable to those for martian meteorite ejection, do not seem to be an obstacle for the survival of microorganisms, as has been convincingly demonstrated by Mastrapa *et al.* (2001) and Benardini *et al.* (2003). We have, therefore, concentrated on studying the lethal influence of the impact-associated pressure-temperature (*P-T*) history on microorganisms embedded within silicate rocks similar to those of the martian crust.

The general assessment of the *P-T*-time profiles expected in martian meteorites reveals the following facts:

(a) Martian meteorites were affected by shock pressures in the range from about 5–55 GPa. The different lithological groups display distinctly different ranges of shock pressures (Table 4) with a typical pressure of <35 GPa for the pyroxenites and dunites and a subgroup of the basalts.
(b) The shock temperature increases (Table 4) derived for this pressure range are of extremely short duration, as are the peak pressures, *i.e.*, in the order of microseconds for projectiles of several 100 m in diameter.
(c) The post-shock temperature increases calculated for the above pressure range vary from a minimum of 1 K to a maximum of 1000 K (Table 4, Fig. 17). The duration of the temperature depends on the size of the ejected rock fragment and its cooling in space. For the inner part of a spherical rock of 1 or 0.5 m in diameter, it may take 3 or 0.5 h, respectively, to reach the low temperature of the space environment. Table 4 shows that the 5 lithological types of martian meteorites were affected by drastically different post-shock temperatures (and shock pressures) and only about 45% of all martian meteorites experienced temperature increases above about 150 K.

These empirical data of martian meteorites have been confirmed by theoretical models and detailed computer code calculations for the impact and ejection mechanism, the *P-T* conditions, and the source region in the impacted target (Melosh, 1984; Vickery and Melosh, 1987; Head *et al.*, 2002; Artemieva and Ivanov, 2004; Fritz *et al.*, 2005). Model calculations show that, among all fragments ejected at velocities >5 km/s, only a small fraction (about 5–10%) experienced pressures <10 GPa, whereas the mass of ejected rocks were shocked at higher pressures, *e.g.*, 30–40% were highly shocked (about 30–40 GPa) (Artemieva, unpublished data). These theoretical estimates are very much compatible with the shock intensity data of the presently known population of about 40 martian meteorites: the percentage of martian meteorites shocked in the range of 30–40 GPa is about 33%, and the percentage of those shocked to about 10 GPa is about 10% (Fritz *et al.*, 2005; Meyer, 2006)

In our shock recovery experiments, we chose the exact pressure range (5–50 GPa) experienced by martian meteorites to study systematically the effects of a simulated impact event on rock-colonizing microorganisms (Fig. 17). Such shock recovery devices have proved, over the years, to be valuable with regard to the simulation of impact-induced shock metamorphism of rocks and minerals (*e.g.*, Müller and Hornemann, 1969; Stöffler and Langenhorst, 1994). Until now, they have provided the best possible simulation of conditions that prevail in microbe-loaded rocks during small-scale impacts on planetary surfaces. Among all essential parameters, the peak shock pressure P and the pre-impact temperature T_0 of natural events can be tested most realistically, whereas the *P-T*-time profiles of natural impacts are somewhat different from those of the recovery experiments (Fig. 18). The duration of the peak pressures and, consequently, the shock temperatures was distinctly lower in our experiments (by about 1 order of magnitude) as was the magnitude of the shock and post-shock temperatures (compare Table 2 with Table 4; Fig. 18). In addition, the temperature-time profile of the experiments is different from natural events due to the experimental setup and the reverberation technique. The temperature experienced by the layer of microorganisms rose from the initial room temperature T_0 to the shock temperature T_2 of the gabbro, which experienced a very short thermal peak T_1 (see values in Table 3), then fell to the

Table 4. Shock Pressure Range Observed in Various Types of Martian Meteorites, Calculated Shock (T_s) and Post-shock (T_{ps}) Temperature Increase, and Average Plagioclase Content

	Post-shock temperature increase ΔT *[K]*											
	Nakhlites (clinopyroxenites)		*Chassignites (dunites)*		*Orthopyroxenite ALH 84001*		*Basaltic shergottites*		*Olivine-phyric shergottites*		*Lherzolitic shergottites*	
Shock pressure [GPa]	T_s	T_{ps}	T_s	T_{ps}	T_s	T_{ps}	T_s	T_{ps}	T_s	T_{ps}	T_s	T_{ps}
5–20	5–30	1–30										
26–32			60–80	40–70								
31–33					140–160	100–110						
28–33[a]							220–320	70–120				
20–29[b]									30–300	25–70		
42–48[c]							860–1300	440–680				
40–45[d]									600–950	400–500		
40–55											750–1500	370–1000
Plagioclase content (vol. %)	9		1		2		25[a] 45[b]		15		5	

Shock temperatures from Fritz (2005) after a method described by Schmitt (2000); post-shock temperatures from Fritz *et al.* (2005) and average plagioclase content from Meyer (2006).

[a]Zagami and Shergotty.

[b]Y-980459 and Dhofar 019.

[c]QUE 94201 and Los Angeles.

[d]DaG 476 and SaU 005.

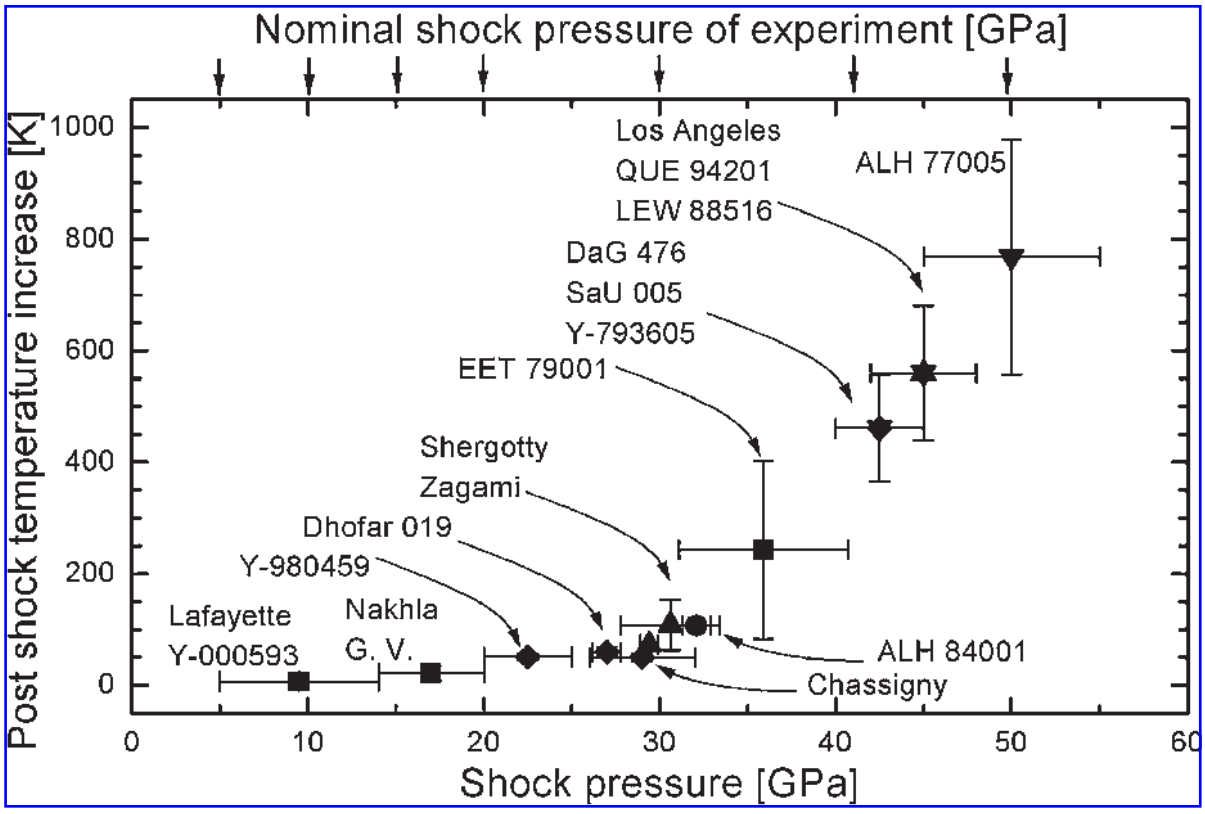

FIG. 17. Calculated post-shock temperatures of 17 different martian meteorites as a function of shock pressure determined in these meteorites on the basis of shock effects in plagioclase (refractive index), pyroxene and olivine (modified after Fritz *et al.*, 2005) and nominal shock pressures of the experiments. Error bars are given for both shock temperature and shock pressure.

post-shock temperature T_3 (both different in iron and in microbe-loaded gabbro), rose again to the equilibration post-shock temperature T_4, and finally reached the "quenching" temperature T_5, which was achieved by the cooling of the recovered shock-heated iron container. This temperature-time relationship is schematically shown in Fig. 18 in comparison with a natural temperature-time-profile. Absolute values for P and T are given in Tables 2 and 3.

The described quantified experimental conditions, in which a realistic martian analogue rock was used as the host rock and the full pressure range observed in martian meteorites (Table 4) was covered, have not previously been applied systematically to microorganisms, though other types of shock experiments with microbes have been performed (*e.g.*, Burchell *et al.*, 2004; Willis *et al.*, 2006). When comparing our results to those in the literature, we must distinguish between 2 types of shock experiment that involve microorganisms as targets. In the first type of experiment, which is qualitatively applicable to martian con-

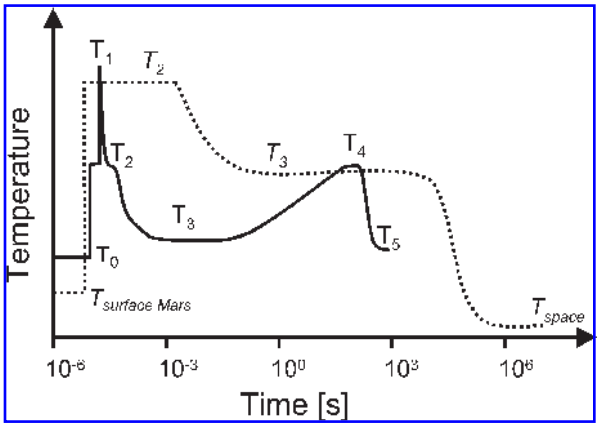

FIG. 18. Schematic temperature-time path (solid line) for the microbial layer during the shock reverberation experiments compared with a typical path for a martian meteorite (dashed line). T_0 = pre-shock ambient temperature; T_1 = initial shock temperature of the microbial layer; T_2 = equilibrium shock temperature in gabbro and microbial layer; T_3 = post-shock temperature of gabbro and microbial layer; T_4 = equilibrium temperature of iron container, gabbro, and microbial layer; T_5 = final temperature after quenching to ambient temperature.

ditions, silicate host materials loaded with microorganisms are impacted by projectiles. Horneck *et al.* (2001b) exposed spores of *B. subtilis* that were encased between quartz plates to a planar shock wave of 32 GPa—a typical pressure recorded in basaltic meteorites from Mars—and found a survival rate of 10^{-4}. Nicholson *et al.* (2006) impacted Al projectiles at 5.4 km/s into granite targets loaded with *B. subtilis* spores and found surviving spores in ejected granite fragments. To date, however, it has not been possible to determine the exact shock pressure experienced by the microorganisms (probably <10 GPa). In a second type of shock experiment, microorganisms were embedded in non-silicate targets. Burchell *et al.* (2001, 2003, 2004) impacted porous ceramic projectiles infused with microorganisms (*Rhodococcus erythopholis* or spores of *B. subtilis*) on targets of nutrient agar or ice. The investigators observed survival rates of 10^{-4} to 10^{-8} in the 3–78 GPa pressure range. The Burchell *et al.* studies were mainly targeted toward the icy satellites of the giant planets and the possible transfer of life between them. In fact, the applied maximum shock pressures of 78 GPa would lead to a complete melting of basaltic rocks. Willis *et al.* (2006) treated aqueous suspensions of *Escherichia coli* cells encased in an iron container by plane shock waves of low pressure (220 and 260 MPa), which are an order of magnitude lower than needed for impact ejection of rock fragments from Mars. The observed survival rates of $>10^{-4}$ were, however, applicable to conditions of early Earth and assessment of the subsurface microbial mortality after giant impacts.

The organisms selected for our studies can be considered model systems for potential "hitchhikers" within impact-ejected rocks. *Bacillus* spores were found to inhabit surface basalts (Benardini *et al.*, 2003) and near-subsurface granite, though their concentration (<500/g) was lower than that of total viable bacteria (Nicholson *et al.*, 2006). Because they are widely accepted as the hardiest microbial representatives that can withstand extreme environmental stress conditions, *Bacillus* spores are the most frequently used test objects in experiments in space as well as in ground-based simulations for studying the different steps of lithopanspermia (Burchell *et al.*, 2004; Fajardo-Cavazos *et al.*, 2005; Nicholson and Schuerger, 2005; reviewed in Horneck, 1993; Nicholson *et al.*, 2000).

We are aware that bacterial endospores, which belong to heterotrophic organisms, are not well suited as first colonizers on a planet barren of indigenous life unless they were delivered to a pond enriched with organics (*e.g.*, primordial soup). Therefore, we have extended our studies to 2 rock-colonizing autotrophic organisms—the endolithic cyanobacterium *Chroococcidiopsis* and the epilithic symbiotic system *Xanthoria elegans*. Both systems have demonstrated a high resistance to the certain parameters of space (de Vera *et al.*, 2003, 2004; Sancho *et al.*, 2007) as well as to martian surface conditions (Cockell *et al.*, 2005).

Our systematic shock recovery experiments are the first to have produced "dose-effect curves" for the 3 groups of microorganisms over a pressure range relevant for martian meteorites. For the interpretation of the observed effects, the special *P-T*-time conditions imposed by the high-explosive setup and the reverberation technique on the microorganisms encased in the gabbro sandwich should be kept in mind (see first part of this section and Sections 2.1 and 3.2.). We identified 3 critical parameters that potentially affect survival of the microorganisms: namely, the shock pressure, the various temperature increases, and the duration of these factors. The most effective characteristics of the temperature-time profiles (Tables 2 and 3 and Fig. 18) are, first, a rather high but extremely short (< about 1 μs) shock temperature spike (T_1) in the microbial layer and, second, a moderately high final equilibrium post-shock temperature (T_4) after heat exchange between iron and gabbro. ΔT_4 exceeds 100°C only at pressures above about 30 GPa. The shock compression and the post-shock temperatures T_4 were probably the most effective parameters for the survival rates of the microorganisms in our experiments. Moreover, we have overestimated the thermal spike T_1 because the density of the microbial layer was higher (*e.g.*, 1.3 g/cm^3 for *B. subtilis* spores) than that of pure water.

B. subtilis spores, which are dormant and exhibit incredible longevity and resistance to environmental extremes, were rarely affected at shock pressures of 10 GPa or less and survived treatments up to 41.5 GPa (survival rate 10^{-4}). No survivors were recorded at 50 GPa with a detection limit of 5×10^{-8}. These data agree with those of our earlier studies on spores that were sandwiched between quartz discs and exposed to a shock pressure of 32 GPa (Horneck *et al.*, 2001b). Our data demonstrate the high resistance of bacterial spores to impact events. This resistance is

probably due to the spore coatings and the rigid cortex that protects the core during the process of shock compression. Furthermore, the mineralized and dehydrated spore core, with the DNA well protected, enables bacterial spores to survive extremely high temperatures, *e.g.*, 150°C for 1 h (Nicholson *et al.*, 2000). Therefore, we suggest that the spores can tolerate high temperature peaks that last only for microseconds without significant damage. However, it may be the combined effect of all factors that determine the *P-T*-time profile that leads to inactivation of the spores at higher shock pressures. Therefore, the high temperature peaks lasting for microseconds only are suggested to be tolerated by the spores without remarkable damage. However, it may finally be the interplay of all factors determining the *P-T*-time profile that lead to inactivation of the spores at higher shock pressures.

The lichen *Xanthoria elegans* was also highly resistant to the shock-wave treatment, as determined separately for the photobiont and mycobiont. In general, the vegetative mycobiont exhibited pressure-effect curves similar to those determined for the survival of *B. subtilis* spores. The generative ascospores were even more resistant, some being vital after treatment at 50 GPa, the highest pressure applied. It should be noted, however, that the vitality tests determined by live/dead staining with CLSM applied for the lichens is different from the survival test used for bacterial spores. While the first test gives information as to whether the membranes as well as the physiological processes of the cells are intact, the latter test indicates the presence of actively dividing cells capable of forming colonies. The physiological activity in the lichen is reflected by color changes of the plasma and is caused by transport processes from the cell plasma into vacuoles and vesicles, where the reaction products with the staining substances (red crystals) are deposited.

In their natural environment, lichens on rocks can reach quite high temperatures at noon during summer, which, until the rocks cool later in the day, can last for several hours (de la Torre *et al.*, 2007). Therefore, the peak temperature increases experienced for microseconds or less during the shock recovery experiments are probably not of great harm to the lichens. It is interesting to note that, for low pressures (<20 GPa), the degree of damage observed in the lichen thalli was highest in the center of the disc and declined gradually to the rim. This might be an indication that the lichen is a more sensitive bioindicator for shock pressures than the rock itself, for which no variation of shock pressures over the disc was detected.

Chroococcidiopsis sp. was found to be susceptible to high shock pressures. At pressures greater than 10 GPa, the cells were lysed and their contents dispersed. From the *P-T*-time profile, 2 potential causes of this effect must be considered. High temperatures may have caused cell lysis. However, cells exposed to high temperatures alone become small and shriveled (data not shown) rather than ruptured. We attribute the rupturing to high shock pressures that exceed the dynamic tensile cell wall strength of the cyanobacterial cell wall. These data are consistent with that of Willis *et al.* (2006), who showed that even moderate shock pressures caused cell wall indentation in *E. coli* cells. They concluded that cell wall strength was the critical failure mode for these cells. Although our vegetative cells have a thick cyanobacterial sheath, the typical size of *Chroococcidiopsis* is 2 to 4 times that of *E. coli*, which is likely to make them more susceptible to high shock pressures and physical sheering caused by rock displacement. Like many material failure modes, our data could mean that cells reached a critical strength failure at a pressure between 10 and 20 GPa, which causes catastrophic failure of the cell walls. These data are consistent with Willis *et al.* (2006) and suggest that a simple logarithmic decline in cell viability—similar to that, for example, for the effects of UV radiation on cell viability—contributes little to our understanding of microbial response to impact shock pressures. Rather, a more physical model of material failure modes would be more appropriate.

5. CONCLUSIONS

In addition to our study of prokaryotic organisms, we are the first to have extended impact simulation shock-wave experiments to the study of photosynthetic organisms and, particularly, eukaryotes and complex eukaryotic symbiotic systems. The vital launch window for the transport of rock-colonizing microorganisms from a Mars-like planet depends on the physiological states of the microorganisms. It encompasses shock pressures in the range of 5 to about 40 GPa for bacterial endospores and lichens, and is lim-

ited to shock pressures from 5–10 GPa for the cyanobacteria. This vital launch window is in accordance with the total launch window of martian meteorites, which is from 5–10 GPa to 50–55 GPa. Hence, the results of our systematic shock recovery experiments give further support to the hypothesis of lithopanspermia for a viable transport from Mars to Earth or from any Mars-like planet to another habitable planet in the same stellar system. Considering the low frequency of weakly shocked meteorites (about 5% with pressures of <10 GPa in the case for Mars), however, this fact further reduces the chances for interplanetary transport of cyanobacteria-type organisms.

A vital launch window for the escape from Earth's gravity field may only be achieved by very large impact events that blow out at least part of the atmosphere (Gladman *et al.*, 2005; Wells *et al.*, 2003). The direct ejection and escape of rocks from Earth is very difficult because of the required very high escape velocity (11 km/s) and the decelerating effect of Earth's dense atmosphere. Therefore, "mega-impacts," which occurred frequently only during the "early heavy bombardment phase," *i.e.*, before 3.75 billion years ago (*e.g.*, Jolliff *et al.*, 2006), would be required to transfer sufficiently large fragments of moderately shocked rocks into space. Our results enlarge the number of potential organisms that might be able to reseed a planetary surface after "early," very large impact events (Wells *et al.*, 2003) and suggest that such a re-seeding scenario on a planetary surface is possible with diverse organisms.

APPENDIX

Reverberation technique

In the reverberation technique the peak shock pressure in the sample is achieved via multiple reflections of the shock wave at the metal container-rock interfaces (*e.g.*, Müller and Hornemann, 1969; Stöffler and Langenhorst, 1994; Horneck *et al.*, 2001b). For a better understanding of the pressure-temperature-time history of the shocked samples, some details of the experimental technique are given. All metal parts in this device consist of steel (ARMCO iron). A metal plate, the flyer plate, is attached to the high explosive and is kept a short distance above the upper surface of the sample container by means of a (soft) plastic ring. The flyer plate has a thickness *d*. The sample consists of a layer of microorganisms sandwiched between two 0.5 mm thick discs of rock. It is positioned on top of a cylindrical inner sample container at a depth *D* from the surface and is surrounded by an outer sample container that protects the inner container holding the sample from breaking apart upon detonation of the high explosive. The desired peak shock pressure, which is produced by the impact of the flyer plate, can be varied by changing the values of *d* and *D* or the type of explosive. If *d* is decreased, the impact velocity increases and, hence, a higher shock pressure will be achieved in the sample. If *D* is increased, the shock pressure in the sample will be lower because the shock wave running downward from the top of the container loses energy while propagating into the steel container. The correlation between *d, D,* and the shock pressure has to be calibrated with electrical pins as a function of the type of explosive (see details in Müller and Hornemann, 1969).

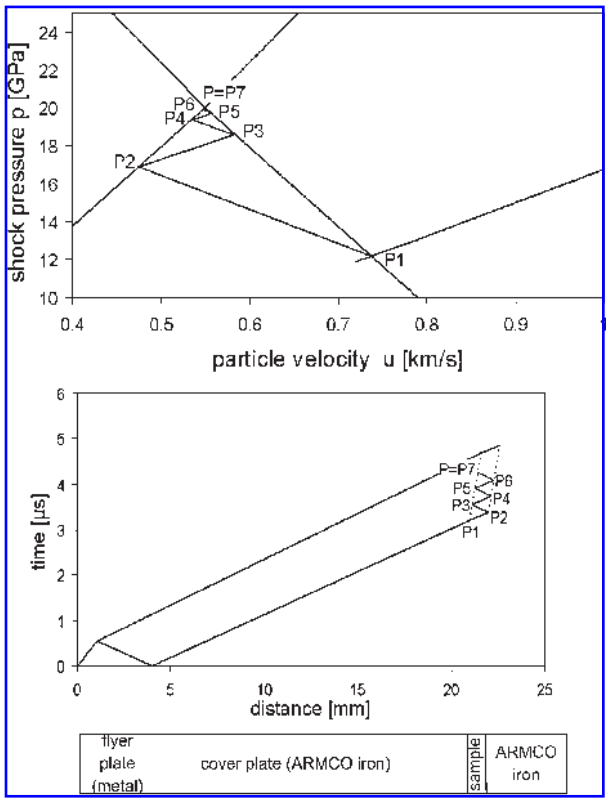

FIG. A1. Time-distance plot for the propagating shock wave(s) in the iron-gabbro-microbe–layer setup of a shock recovery experiment with a nominal shock pressure of 20 GPa.

We consider a typical shock recovery experiment, in which a 1.0 mm thick disc of gabbro is shocked to 20 GPa. The detonation of the high explosive accelerates the plate of ARMCO iron of thickness $d = 4$ mm to a velocity of 1.89 km/s impacting the plane surface of the iron container where the rock disc is located at a depth $D = 17$ mm. The shock wave, which arrives at the upper iron-rock interface with a pressure $P = 20$ GPa, propagates into the rock and decreases its pressure to $P_1 = 12.2$ GPa because of the lower shock impedance of gabbro (shock impedance = density of gabbro at zero pressure times shock velocity). The 12.2 GPa shock is reflected at the lower interface of gabbro and iron and runs back into the gabbro as a shock wave of increased pressure $P_2 = 16.9$ GPa, which then gets reflected back again into the gabbro at the upper contact of gabbro and iron, thereby increasing the pressure to $P_3 = 18.6$ GPa. These reverberations and stepwise increases of pressure continue until the rarefaction wave reflected back from the impacted flyer plate arrives at the gabbro sample, thereby releasing the sample from the compressed state. Appendix Fig. A1 shows that the peak pressure P_7 (= 19.94 GPa), which is virtually identical to the starting pressure $P_0 = 20.0$ GPa, is reached after 6 reverberations, *i.e.,* after 4.26 μs, long before the rarefaction wave arrives after 4.85 μs. This means that the peak pressure duration (pulse length) in gabbro is 0.59 μs in this experiment. It should be pointed out here that there is a special effect of the 1–50 μm thick microbial layer on the pressure-temperature history of the microorganisms because of their low density and therefore low shock impedance.

6. ACKNOWLEDGMENTS

This work was supported by the Deutsche Forschungsgemeinschaft (HO 1508/3-1 to G. Horneck; STO 101/39-1 to D. Stöffler) within the DFG Priority Program "Mars and terrestrial planets", and by a grant of the Bundesministerium für Wirtschaft und Technologie through DLR (BMWi, 50WB0614 to S. Ott and J.P. de Vera) within the ESA projects "Lithopanspermia" and "LIFE." We thank Hendryk Schneider, Hans-Rudolf Knöfler, Simon Jokisch, and Hartmut Friedrich for skillful technical assistance during the construction and recovery of the experiment hardware and Heiko Will for assisting with the high-explosive experiments.

7. ABBREVIATIONS

An, anorthite; CLSM, confocal laser scanning microscope; RIs, refractive indices.

8. REFERENCES

Arnold, W. (1988) Dynamisches Materialverhalten von Armco-Eisen, -Experiment und Simulation, EMI-FhG Bericht E 30/88, Fraunhofer Gesellschaft, Freiburg, Germany.

Arrhenius, S. (1903) Die Verbreitung des Lebens im Weltenraum. *Die Umschau* 7, 481–485.

Artemieva, N.A. and Ivanov, B.A. (2004) Launch of martian meteorites in oblique impacts. *Icarus* 171, 183–196.

Baltschukat, K. and Horneck, G. (1991) Responses to accelerated heavy ions of spores of *Bacillus subtilis* of different repair capacity. *Radiat. Environ. Biophys.* 30, 87–103.

Belnep, J., Büdel, B., and Lange, O.L. (2001) Biological soil crusts: characteristics and distribution. *Ecological Studies* 150, 3–31.

Benardini, J.N., Sawyer, J., Venkateswaran, K., and Nicholson, W.L. (2003) Spore UV and acceleration resistance of endolithic *Bacillus pumilus* and *Bacillus subtilis* isolates obtained from Sonoran desert basalt: implications for lithopanspermia. *Astrobiology* 3, 709–717.

Berlin, E., Curran, H.R., and Pallansch, M.J. (1963) Physical surface features and chemical density of dry bacterial spores. *J. Bacteriol.* 86, 1030–1036.

Bischoff, A. and Stöffler, D. (1992) Shock metamorphism as a fundamental process in the evolution of planetary bodies: information from meteorites. *Eur. J. Mineral.* 4, 707–755.

Büdel, B. and Wessels, D.C.J. (1991) Rock inhabiting blue-green algae/cyanobacteria from hot arid regions. *Algal Studies* 64, 385–398.

Burchell, M.J., Mann, J., Bunch, A.W., and Brandao, P.F.B. (2001) Survivability of bacteria in hypervelocity impact. *Icarus* 154, 545–547.

Burchell, M.J., Galloway, J.A., Bunch, A.W., and Brandao, P.F.B. (2003) Survivability of bacteria ejected from icy surfaces after hypervelocity impact. *Orig. Life Evol. Biosphere* 33, 53–74.

Burchell, M.J., Mann, J.R., and Bunch, A.W. (2004) Survival of bacteria and spores under extreme shock pressures. *Mon. Not. R. Astron. Soc.* 352, 1273–1278.

Clark, B.C. (2001) Planetary interchange of bioactive material: probability factors and implications. *Orig. Life Evol. Biosphere* 31, 185–197.

Cockell, C.S., Schuerger, A.C., Billi, D., Friedmann, E.I., and Panitz, C. (2005) Effects of a simulated martian UV flux on the cyanobacterium *Chroococcidiopsis* 029. *Astrobiology* 5, 127–140.

Cockell, C.S., Koeberl, C., and Gilmour, I., editors. (2006) *Biological Processes Associated with Impact Events.* Springer, Berlin.

DeCarli, P.S., Bowden, E., Jones, A.P., and Price, G.D. (2002) Laboratory impact experiments versus natural

impact events. In *Catastrophic Events and Mass Extinctions, Geol. Soc. America Special Paper 356,* edited by C. Köberl and K.G. MacLeod, The Geological Society of America, Boulder, CO, pp. 595–606.

de la Torre, R., Horneck, G., Sancho, L.G., Scherer, K., Facius, R., Urlings, T., Rettberg, P., Reina, M., and Pintado, A. (2002) Photoecological characterization of an epilithic ecosystem at high mountain locality (central Spain). In *Proceedings of the Second European Workshop on Exo/Astrobiology*, edited by H. Lacoste, ESA SP-518, ESA-ESTEC, Noordwijk, the Netherlands, pp. 443–444.

de la Torre, R., Garcia-Sancho, L., and Horneck, G. (2007) Adaptation of the lichen *Rhizocarpon geographicum* to harsh high altitude conditions: relevance to a habitable Mars. In *Responses of Organisms to Simulated Mars Environment (ROME)*, edited by C.S. Cockell and G. Horneck, ESA-SP 1299, ESA Publications Division, ESTEC, Noordwijk, the Netherlands, pp. 145–150.

de Vera, J.P., Horneck, G., Rettberg, P., and Ott, S. (2003) The potential of lichen symbiosis to cope with extreme conditions of outer space. I. Influence of UV radiation and space vacuum on the vitality of lichen symbiosis and germination capacity. *Int. J. Astrobiol.* 1, 285–293.

de Vera, J.P., Horneck, G., Rettberg, P., and Ott, S. (2004) The potential of lichen symbiosis to cope with the extreme conditions of outer space. II. Germination capacity of lichen ascospores in response to simulated space conditions. *Adv. Space Res.* 33, 1236–1243.

Eugster, O., Weigel, A., and Polnau, E. (1997) Ejection times of martian meteorites. *Geochim. Cosmochim. Acta* 61, 2749–2757.

Fajardo-Cavazos, P., Link, L., Melosh, H.J., and Nicholson, W.L. (2005) *Bacillus subtilis* spores on artificial meteorites survive hypervelocity atmospheric entry: implications for lithopanspermia. *Astrobiology* 5, 726–736.

Flemming, H.C. and Wingender, J. (2001) Biofilme—die bevorzugte Lebensform der Bakterien. *Biologie in unserer Zeit* 3, 169–180.

Friedmann, E.I. and Ocampo-Friedmann, R. (1985) Bluegreen algae in arid cryptoendolithic habitats. *Archiv für Hydrobiologie* 38/39, 349–350.

Fritz J. (2005) Aufbruch vom Mars: Petrographie und Stoßwellenmetamorphose von Marsmeteoriten. Mathematisch-Naturwissenschaftliche Fakultät I, Humboldt-Universität zu Berlin, p. 138.

Fritz, J., Greshake, A., Stöffler, D., and Hecht, L. (2002) Shock metamorphism of martian meteorites: new data from quantitative shock pressure barometry [abstract 1504]. In *33rd Lunar and Planetary Science Conference Abstracts,* LPI Contribution No. 1109, Lunar and Planetary Institute, Houston.

Fritz, J., Artemieva, N.A., and Greshake, A. (2005) Ejection of martian meteorites. *Meteorit. Planet. Sci.* 40, 1393–1411.

Gladman, B. (1997) Destination: Earth. Martian meteorite delivery. *Icarus* 130, 228–246.

Gladman, B., Dones, L., Levison, H.F., and Burns, J.A. (2005) Impact seeding and reseeding in the inner Solar System. *Astrobiology* 5, 483–496.

Golubic, S., Friedmann, E.I., and Schneider, J. (1981) The lithobiontic ecological niche, with special reference to microorganisms. *J. Sediment. Petrol.* 51, 475–478.

Green, T.G.A., Schroeter, B., and Sancho, L.G. (1999) Plant life in Antarctica. In *Handbook of Functional Plant Ecology*, edited by F.I. Pugnaire and F. Valladares, Marcel Dekker, New York, pp. 495–543.

Grilli Caiola, M., Ocampo-Friedmann, R., and Friedmann, E.I. (1993) Cytology of long-term desiccation in the desert cyanobacterium *Chroococcidiopsis* (Chroococcales). *Phycologia* 32, 315–322.

Head, J.N., Melosh, H.J., and Ivanov, B.A. (2002) Martian meteorite launch: high-speed ejecta from small craters. *Science* 298, 1752–1756.

Horneck, G. (1993) Responses of *Bacillus subtilis* spores to space environment: results from experiments in space. *Orig. Life Evol. Biosphere* 23, 37–52.

Horneck, G., Bücker, H., Reitz, G., Requardt, H., Dose, K., Martens, K.D., Mennigmann, H.D., and Weber, P. (1984) Microorganisms in the space environment. *Science* 225, 226–228.

Horneck, G., Bücker, H., and Reitz, G. (1994) Long-term survival of bacterial spores in space. *Adv. Space Res.* 14, 41–45.

Horneck, G., Eschweiler, U., Reitz, G., Wehner, J., Willimek, R., and Strauch, K. (1995) Biological responses to space: results of the experiment "Exobiological Unit" of ERA on EURECA I. *Adv. Space Res.* 16, 105–118.

Horneck, G., Rettberg, P., Reitz, G., Wehner, J., Eschweiler, U., Strauch, K., Panitz, C., Starke, V., and Baumstark-Khan, C. (2001a) Protection of bacterial spores in space, a contribution to the discussion on panspermia. *Orig. Life Evol. Biosphere* 31, 527–547.

Horneck, G., Stöffler, D., Eschweiler, U., and Hornemann, U. (2001b) Bacterial spores survive simulated meteorite impact. *Icarus* 149, 285–293.

Joliff, B.L., Wieczorek, M.A., Shearer, C.K. and Neal, C.R., editors. (2006) *New Views of the Moon: Reviews in Mineralogy and Geochemistry,* Vol. 60*,* Mineralogical Society of America and The Geochemical Society, The Mineralogical Society of America, Chantilly, Virginia.

Kleber, W. (1970) *An Introduction to Crystallography.* VEB Verlag Technik, Berlin.

Komárek, J. and Anagnostidis, K. (1998) *Xenococcaceae.* In *Süßwasserflora von Mitteleuropa. Cyanoprokaryota: Chroococcales*, edited by H. Ettl, J. Gerloff, H., Heynig, and D. Mollenhauer, Gustav Fischer Verlag, Germany, pp. 419–441.

Kranner, I., Cram, W.J., Zorn, M., Wornik, S., Yoshimura, I., Stabentheiner, E., and Pfeifhofer, H.W. (2005) Antioxidants and photoprotection in a lichen as compared with its isolated symbiotic partners. *Proc. Natl. Acad. Sci. U.S.A.* 102, 3141–3146.

Maher, K.A. and Stevenson, D.J. (1988) Impact frustration of the origin of life. *Nature* 331, 612–614.

Mancinelli, R.L., White, M.R. and Rothschild, L.J. (1998) Biopan survival. I. Exposure of the osmophiles *Synechococcus sp*. (Nageli) and *Haloarcula sp.* to the space environment. *Adv. Space Res.* 22, 327–334.

Mastrapa, R.M.E., Glanzberg, H., Head, J.N., Melosh, H.J., and Nicholson, W.L. (2001) Survival of bacteria exposed to extreme acceleration: implications for panspermia. *Earth Planet. Sci. Lett.* 189, 1–8.

McQueen, R.G. and Marsh, S.P. (1960) Equation of state for nineteen metallic elements from shock-wave measurements to two megabars. *J. Appl. Phys.* 31, 1253–1269.

Melosh, H.J. (1984) Impact ejection, spallation, and the origin of meteorites. *Icarus* 59, 234–260.

Melosh, H.J. (1988) The rocky road to panspermia. *Nature* 332, 687–688.

Meyer, C. (2006) The Mars Meteorite Compendium, Astromaterials Research and Exploration Science (ARES), (JSC #27672 Revision C), Lyndon B. Johnson Space Center, Houston, Texas. Available online at http://curator.jsc.nasa.gov/antmet/mmc/index.cfm

Mileikowsky, C., Cucinotta, F., Wilson, J.W., Gladman, B., Horneck, G., Lindegren, L., Melosh, J., Rickman, H., Valtonen, M., and Zheng, J.Q. (2000) Natural transfer of viable microbes in space. 1. From Mars to Earth and Earth to Mars. *Icarus* 145, 391–427.

Müller, W.F. and Hornemann, U. (1969) Shock-induced planar deformation structures in experimentally shock-loaded olivines and in olivines from chondritic meteorites. *Earth Planet. Sci. Lett.* 7, 251–264.

Nicholson, W.L. and Schuerger, A.C. (2005) *Bacillus subtilis* spore survival and expression of germination-induced bioluminescence after prolonged incubation under simulated Mars atmospheric pressure and composition: implications for planetary protection and lithopanspermia. *Astrobiology* 5, 536–544.

Nicholson, W.L., Munakata, N., Horneck, G., Melosh, H.J., and Setlow, P. (2000) Resistance of bacterial spores to extreme terrestrial and extraterrestrial environments. *Microbiol. Mol. Biol. Rev.* 64, 548–572.

Nicholson, W.L., Fajardo-Cavazos, P., Langenhorst, F., and Melosh, H.J. (2006) Bacterial spores survive hypervelocity launch by spallation: implications for lithopanspermia [abstract 1808]. In *37th Lunar and Planetary Science Conference Abstracts*, LPI Contribution No. 1303, Lunar and Planetary Institute, Houston.

Nyquist, L.E., Bogard, D.D., Shih, C.-Y., Greshake, A., Stöffler, D., and Eugster, O. (2001) Ages and geological histories of martian meteorites. *Space Sci. Rev.* 96, 105–164.

Reimold, W.U. and Stöffler, D. (1978) Experimental shock metamorphism of dunite. In *Proceedings of the 9th Lunar and Planetary Science Conference*, Vol. 2, New York, Pergamon Press, pp. 2805–2824.

Rippka, R., Deruelles, J., Waterbury, J.B., Herdman, M., and Stanier, R.Y. (1979) Generic assignments, strain histories and properties of pure cultures of cyanobacteria. *J. Gen. Microbiol.* 111, 1–61.

Ryder, G., Fastovsky, D., and Gartner, S., editors. (1996) *The Cretaceous-Tertiary Event and Other Catastrophes in Earth History, Geological Society of America Special Paper 307,* The Geological Society of America, Boulder, CO.

Sancho, L.G., de la Torre, R., Horneck, G., Ascaso, C., de los Rios, A., Pintado, A., Wierzchos, J., and Schuster, M. (2007) Lichens survive in space. *Astrobiology* 7, 443–454.

Schaeffer, P., Millet, J., and Aubert, J.P. (1965) Catabolic repression of bacterial sporulation. *Proc. Natl. Acad. Sci. U.S.A.* 54, 704–711.

Schmitt, R.T. (2000) Shock experiments with the H6 chondrite Kernouvé: pressure calibration of microscopic shock effects. *Meteorit. Planet. Sci.* 35, 545–560.

Setlow, P. (1994) Mechanisms which contribute to the long-term survival of spores of *Bacillus* species. *J. Appl. Bacteriol.* 76, 49S–60S.

Sleep, N.H. and Zahnle, K. (1998) Refugia from asteroid impacts on early Mars and the early Earth. *J. Geophys. Res.* 103, 28529–28544.

Sleep, N.H., Zahnle, K., Kasting, J., and Morowitz, H. (1989) Annihilation of ecosystems by large asteroid impacts on the early Earth. *Nature* 342, 139–142.

Solhaug, K.A. and Gauslaa, Y. (2004) Photosynthates stimulate the UV-B induced fungal anthraquinone synthesis in the foliose lichen *Xanthoria parietina*. *Plant Cell Environ.* 27, 167–176.

Solhaug, K.A., Gauslaa, Y., Nybakken, L., and Bilger, W. (2003) UV induction of sun-screening pigments in lichens. *New Phytol.* 158, 91–100.

Squyres, S.W., Grotzinger, J.P., Arvidson, R.E., Bell, J.F., III, Calvin, W., Christenson, P.R., Clark, B.C., Crisp, J.A., Farrand, W.H., Herkenhoff, K.E., Johnson, J.R., Klingelhöfer, G., Knoll, A.H., McLennan, S.M., McSween, H.Y., Jr., Morris, R.V., Rice, J.W., Jr., Rieder, R., and Soderblom, L.A. (2004) *In situ* evidence for an ancient aqueous environment at Meridiani Planum, Mars. *Science* 306, 1709–1714.

Stewart, S.T. and Ahrens, T.J. (2005) Shock properties of H_2O ice. *J. Geophys. Res.* 110, EO3005.

Stöffler, D. (1984) Glasses formed by hypervelocity impact. *J. Non-Crystalline Solids* 67, 465–502.

Stöffler, D. and Hornemann, U. (1972) Quartz and feldspar glasses produced by natural and experimental shock. *Meteoritics* 7, 371–394.

Stöffler, D. and Langenhorst, F. (1994) Shock metamorphism of quartz in nature and experiment. I. Basic observations and theory. *Meteoritics* 29, 155–188.

Stöffler, D., Ostertag, R., Jammes, C., Pfannenschmitt, G., Sen Gupta, P.R., Simon, S.B., Papike, J.J., and Beauchamp, R.H. (1986) Shock metamorphism and petrography of the Shergotty achondrite. *Geochim. Cosmochim. Acta* 50, 889–903.

Stöffler, D., Keil, K., and Scott, E.R.D. (1991) Shock metamorphism in ordinary chondrites. *Geochim. Cosmochim. Acta* 55, 3845–3867.

Trunin, R.F., Gudarenko, L.F., Zhernokletov, M.V., and Simakov, G.V. (2001) *Experimental Data on Shock Compression and Adiabatic Expansion of Condensed Matter*, Russian Federal Nuclear Center—Vsesoyuznyi Nauchno Issledovatelskyi Institut Experimental'noi Fiziki, Sarov.

Vickery, A.M. and Melosh, H.J. (1987) The large crater origin of SNC meteorites. *Science* 237, 738–743.

Weiss, B.P., Kirschvink, J.L., Baudenbacher, F.J., Vali, H., Peters, N.T., Macdonald, F.A., and Wikswo, J.P. (2000) A low temperature transfer of ALH84001 from Mars to Earth. *Science* 290, 791–795.

Wells, L.E., Armstrong, J.C., and Gonzales, G. (2003) Reseeding of early Earth by impacts of returning ejecta during the Late Heavy Bombardment. *Icarus* 162, 38–46.

Willis, M.J., Ahrens, T.J., Bertani, L.E., and Nash, C.Z. (2006) Bugbuster—survivability of living bacteria upon shock compression. *Earth Planet. Sci. Lett.* 247, 185–196.

Wynn-Williams, D.D., Edwards, H.G.M., Newton, E.M., and Holder, J.M. (2002) Pigmentation as a survival strategy for ancient and modern photosynthetic microbes under high ultraviolet stress on planetary surfaces. *Int. J. Astrobiolol.* 1, 39–49.

Yuan, X., Xiao, S., and Taylor, T.N. (2005) Lichen-like symbiosis 600 Million years ago. *Science* 308, 1017–1020.

Address reprint requests to:
Gerda Horneck
German Aerospace Center DLR
Institute of Aerospace Medicine
D 51170 Köln, Germany

E-mail: gerda.horneck@dlr.de